



TUM School of Life Sciences

Deciphering the role of p53, YAP1 and APC in carcinogenesis. Studies on pig models

Guanglin Niu

Vollständiger Abdruck der von der TUM School of Life Sciences der Technischen Universität München zur Erlangung des akademischen Grades eines Doktors der Naturwissenschaften genehmigten Dissertation.

Vorsitz: Prof. Dr. Benjamin Schusser

Prüfer*innen der Dissertation:

1. Prof. Angelika Schnieke, Ph.D.
2. Prof. Dr. Frank Johannes

Die Dissertation wurde am 20.02.2023 bei der Technischen Universität München eingereicht und durch die TUM School of Life Sciences am 19.05.2023 angenommen.

Abstract

Mutations in tumour suppressor or proto-oncogenes can initiate tumorigenesis in a tissue depended context, e.g. mutations in *KRAS* are driving the development of pancreatic cancer and mutations in *APC* initiate colorectal cancer. *TP53* is the most studied tumour suppressor gene and mutations of p53 are commonly found in various tumours. This thesis aimed to elucidate the molecular basis of tumorigenesis in mutant pigs. Two different porcine cancer models were analyzed; *APC*¹³¹¹ pigs, which develop colon polyposis and mutant *TP53* pigs, which develop osteosarcoma (OS) at high frequency. The latter observation suggested that the dysfunction of *TP53* itself initiates the bone tumorigenesis, but the molecular mechanism was unknown.

In this work, the molecular analysis revealed the presence of two internal *TP53* promoters (P1 and P2) equivalent to those found in human. Similar to humans, pigs also express different *TP53* isoforms. It could be shown that P2-driven expression of the mutant R167H- Δ 152p53 isoform (equivalent to the human R175H- Δ 160p53 isoform) and its circular counterpart *circTP53* determine the tumour spectrum and play a critical role in the malignant transformation in *TP53*^{R167H} pigs. The detection of the Δ 152p53 mRNA isoform in serum was indicative for tumorigenesis. Furthermore, a tissue-specific p53-dependent deregulation of p63 and p73 isoforms in OS was found.

While mutant p53 is essential for OS initiation, other genes play an important role in the disease progression. RNA sequencing and allele expression imbalance (AEI) analysis of OS and matched healthy control samples revealed high significance ($P= 2.14 \times 10^{-39}$) for single nucleotide polymorphisms (SNPs) in the *BIRC3-YAP1* locus. Analysis of copy number variation showed that *YAP1* amplification was associated with the progression of OS. Accordingly, inactivation of *YAP1* inhibits proliferation, migration, invasion and leads to the silencing of *TP63* and reactivation of *p16* expression in *TP53* full-length deficient porcine OS cells. Increased *p16* mRNA expression correlated with lower methylation of its promoter.

In *APC*^{1311/+} pigs, the mutant *APC* 1311 allele induces colon polyposis, which severity varies dramatically between siblings. By using a set of molecular analyses, it could be showed that the level of expression of the wild-type *APC* allele could be responsible for the number of polyps in the colon.

In summary, this work investigated the molecular determinants of cancer in mutant p53 and *APC*¹³¹¹ pigs.

Zusammenfassung

Mutationen in Tumorsuppressoren oder Proto-Onkogenen können die Tumorentstehung in einem gewebeabhängigen Kontext auslösen, z. B. Mutationen in *KRAS* sind für die Entstehung von Bauchspeicheldrüsenkrebs verantwortlich und Mutationen in *APC* lösen Darmkrebs aus. *TP53* ist das am besten untersuchte Tumorsuppressor-Gen, und Mutationen in p53 werden häufig bei verschiedenen Tumoren gefunden. Ziel dieser Arbeit war es, die molekularen Grundlagen der Tumorentstehung bei mutierten Schweinen zu erforschen. Es wurden zwei verschiedene Schweinekrebsmodelle analysiert: Schweine mit mutiertem *TP53*, die Osteosarkome (OS) entwickeln, und Tiere mit *APC 1311 Mutation*, die eine Dickdarmpolyposis entwickeln. Die letztgenannte Beobachtung deutet darauf hin, dass die Funktionsstörung von *TP53* selbst die Knochentumorentstehung auslöst, der molekulare Mechanismus war jedoch unbekannt.

In dieser Arbeit wurden zwei interne *TP53*-Promotoren (P1 und P2) identifiziert, die denen des Menschen entsprechen. Wie bei dem Menschen sind auch bei Schweinen verschiedene p53-Isoformen exprimiert. Es konnte gezeigt werden, dass die P2-gesteuerte Expression der mutierten Isoform R167H-152p53 (entspricht der menschlichen Isoform R175H-160p53) und ihres zirkulären Gegenstücks circTP53 das Tumorspektrum bestimmen und eine entscheidende Rolle bei der malignen Transformation in TP53R167H-Schweinen spielen. Der Nachweis der kürzeren 152p53-Isoform mRNA im Serum konnte als Marker für die Tumorentstehung benutzt werden. Darüber hinaus wurde eine gewebespezifische p53-abhängige Deregulierung der Isoformen p63 und p73 in OS festgestellt.

Während mutiertes p53 für die Entstehung von OS wesentlich ist, spielen andere Gene eine wichtige Rolle bei der Entwicklung der Krankheit. Die Analyse der RNA-Sequenzierung und des Allelexpressionsungleichgewichts (AEI) von OS und angepassten gesunden Kontrollproben ergab eine hohe Signifikanz ($P = 2,14 \times 10^{-39}$) für Einzelnukleotid-Polymorphismen (SNPs) im *BIRC3-YAP1*-Locus. Die Analyse der Kopienzahlvariation zeigte, dass eine YAP1-Amplifikation mit dem Fortschreiten von OS assoziiert war. Dementsprechend hemmt die Inaktivierung von YAP1 die Proliferation, Migration und Invasion und führt zum Silencing von TP63 und zur Reaktivierung der p16-Expression in p53 Vollständigdefiziten OS-Zellen von Schweinen. Eine erhöhte mRNA-Expression von p16 korrelierte mit einer geringeren Methylierung seines Promotors.

Bei *APC*^{1311/+} Schweinen induziert das mutierte *APC* 1311-Allel eine Dickdarmpolyposis, deren Schweregrad zwischen den Geschwistern stark variiert. Mit Hilfe einer Reihe von molekularen Analysen konnte gezeigt werden, dass das Ausmaß der Expression des Wildtyp-APC-Allels für die Anzahl der Polypen im Dickdarm verantwortlich sein könnte.

Zusammenfassend in dieser Arbeit die molekularen Determinanten von Krebs bei Schweinen mit mutiertem p53 und *APC*¹³¹¹ untersucht wurden.

Contents

1.1	<i>TP53</i> gene family.....	8
1.1.1	p53	9
1.1.2	p63	11
1.1.3	p73	12
1.2	<i>YAP1</i> gene	13
1.3	<i>APC</i> gene	14
1.4	Bone cancer	14
1.4.1	Osteosarcoma.....	15
1.4.2	Biology of osteosarcoma.....	15
1.4.2.1	DNA mutations in osteosarcoma	15
1.4.2.1.1	Chromothripsis and Katagis in osteosarcoma.....	15
1.4.2.1.2	Cancer driver genes in osteosarcoma	16
1.4.2.2	Epigenetic mechanisms in osteosarcoma	16
1.4.2.3	Non-coding RNAs in osteosarcoma.....	17
1.5	Animal models of osteosarcoma	19
1.5.1	Canine model of osteosarcoma	19
1.5.2	Mouse model of osteosarcoma.....	19
1.5.3	Rat model of osteosarcoma	20
1.5.4	Pig model of osteosarcoma.....	20
1.6	Colorectal cancer.....	21
1.6.1	Biology of colorectal cancer	21
1.6.1.1	Epigenetic regulation in colorectal cancer.....	21
1.6.1.2	Non-coding RNA in colorectal cancer.....	22
1.7	Animal model of colorectal cancer	22
1.7.1	Mouse model of colorectal cancer	22
1.7.2	Rat model of colorectal cancer.....	23
1.7.3	Pig model of colorectal cancer.....	23
1.8	Aim of the thesis.....	23
2.	Materials and Methods.....	24
2.1	Materials	24
2.1.1	Lab equipment	24
2.1.2	Consumables	26
2.1.3	Chemicals	27
2.1.4	Buffer and Solution.....	28
2.1.5	Tissue culture media and buffer.....	29
2.1.6	Kits	30

2.1.7 Enzymes	31
2.1.8 Antibodies	32
2.1.9 Primers.....	32
2.2 Methods.....	36
2.2.1 Molecular biology methods	36
2.2.1.1 Isolation of plasmid DNA from bacteria (E.coli)	36
2.2.1.2 Isolation of mammalian genomic DNA	37
2.2.1.3 Isolation of RNA.....	38
2.2.1.4 DNase treatment.....	38
2.2.1.5 Quantity and Quality check of nucleic acids	39
2.2.1.6 DNA manipulation	39
2.2.2 Microbiological Methods.....	46
2.2.2.1 Bacterial culture	46
2.2.2.2 Conservation of bacterial liquid	46
2.2.2.3 Bacteria transformation.....	46
2.2.2.4 Blue and white colony screening.....	47
2.2.3 Tissue culture methods.....	47
2.2.3.1 Isolation and culture of porcine cells.....	48
2.2.3.2 Freezing of cells	48
2.2.3.3 Thawing of cells.....	49
2.2.3.4 Cell Passage.....	49
2.2.3.5 Cell counting.....	49
2.2.3.6 Cell transfection	49
2.2.3.7 Cell selection	50
2.2.3.8 Cell clone picking.....	50
2.2.3.9 Cell screening.....	51
2.2.3.10 Cells for somatic cell nuclear transfer.....	51
2.2.3.11 Proliferation assay	51
2.2.3.12 Migration and invasion assay	51
2.2.3.13 Luciferase reporter assay	51
2.2.3.14 Immunofluorescence assay.....	52
2.2.4 Biochemical methods.....	52
2.2.4.1 Protein isolation	52
2.2.4.2 Protein concentration measurement.....	53
2.2.4.3 Western blot analysis.....	53
2.2.5 Microscopy	55
2.2.6 Necropsy examination and tumour analysis	55
2.2.7 Data analysis.....	56
2.2.7.1 Statistical Analysis.....	56
2.2.7.2 Gene set enrichment analysis	56

3. Results	57
3.1 Paper I “Porcine model elucidates function of p53 isoform in carcinogenesis and reveals novel <i>circTP53</i> RNA”	57
3.2 Paper II “Allelic expression imbalance analysis identified <i>YAP1</i> amplification in p53-dependent osteosarcoma”	58
3.3 Paper III “Wild-type <i>APC</i> Influences the Severity of Familial Adenomatous Polyposis”	59
4. Discussion	60
4.1 p53 animal model for osteosarcoma study	60
4.2 Correlation between DNA methylation and promoter activity in pig <i>TP53</i>	61
4.3 Roles of $\Delta 152p53\alpha$ isoform in tumorigenesis	62
4.4 Expression of p53 family members in porcine osteosarcoma	62
4.5 Circular <i>TP53</i> expression in pigs	63
4.6 Next-generation sequencing and AEI analysis reveals <i>YAP1</i> function in osteosarcoma	64
4.7 <i>YAP1</i> in osteosarcoma development	64
4.8 Wild-type <i>APC</i> in Familial Adenomatous Polyposis	65
5. Reference	67
ACKNOWLEDGEMENT	76

1. Introduction

Due to the immense economic and social impact of cancer there is a need for novel diagnostic and treatment options, which requires an understanding of the biological mechanisms underlying tumorigenesis. Mutations in tumour suppressor genes such as *TP53* and *APC* are frequent in different types of cancers. Here, mutant *TP53* and *APC* pig models were employed, to gain better understanding of the regulation of bone and colorectal cancer which might lead to breakthrough in cancer treatment in the long run.

1.1 *TP53* gene family

The *TP53* gene family has evolved millions of years ago during the development of multicellular animals [1]. Despite years of intensive research on the *TP53* gene family, novel and interesting observations are continuously being made. The *TP53* family consists of three genes, *TP53*, *TP63* and *TP73* [2]. These three genes share a similar protein domain structure, which includes transactivation, proline-rich, DNA binding and oligomerization domains, and for *TP63* and *TP73*, also a Sterile alpha motif domain (Figure 1.1). The DNA binding domains from these three genes can bind to similar specific DNA sequences and thus regulate the transcription of some identical and distinct genes [2]. The C-terminal domain varies in size, sequence and function and regulates DNA binding and transcription, mediating the inter- or intra- protein functional interactions [3-5]. More than two transcriptional activation domains are encoded by the N-terminal sequence of all these three proteins [2].

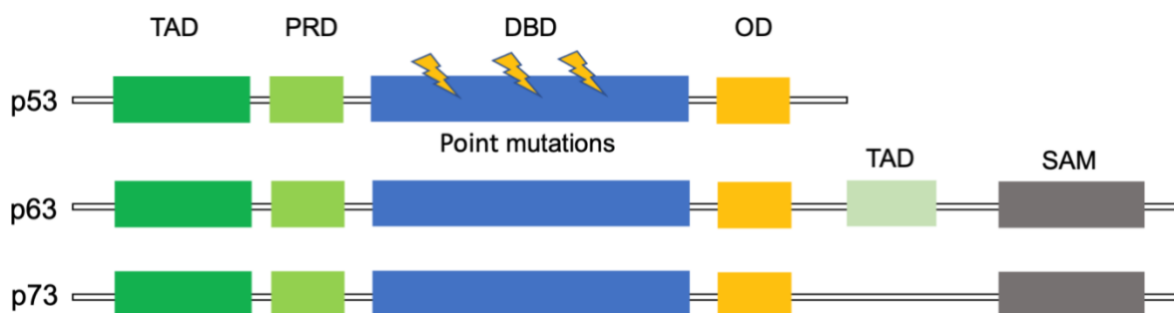


Figure 1.1. Structure of p53 family members Modified from [6]. (TAD: Transactivation domain, PRD: Proline-rich domain, DBD: DNA binding domain, OD: Oligomerization domain. SAM: Sterile alpha motif)

1.1.1 p53

TP53 is commonly mutated in over 50% of human tumours and therefore has been a research focus in cancer biology. It was named “the guardian of the genome”. It functions as a tumour suppressor by regulating cell fate like cell proliferation, differentiation, apoptosis and cell-cycle arrest (Figure 1.2) [7, 8].

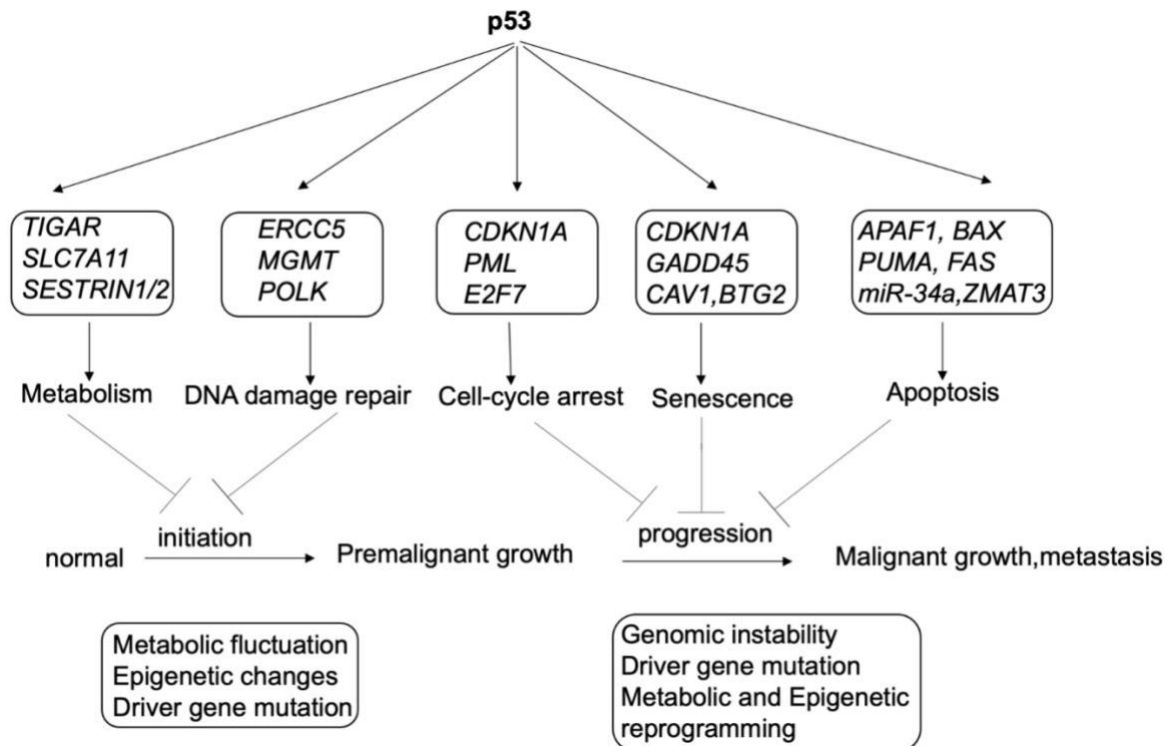


Figure 1.2. Cellular function of p53. Modified from [9, 10]

TP53 gene expression

In human, *TP53* has three promoters (P1 promoter in front of exon 1, Pint1 in intron1 and P2 in intron 4). Nine *TP53* mRNA transcripts which encode at least 12 p53 isoforms (p53 α , p53 β , p53 γ , Δ 40p53 α , Δ 40p53 β , Δ 40p53 γ , Δ 133p53 α , Δ 133p53 β , Δ 133p53 γ , Δ 160p53 α , Δ 160p53 β , Δ 160p53 γ) are expressed in human tissues (Figure 1.3) [11]. Truncated p53 isoforms have been shown to have various functions under normal healthy conditions, including the regulation of gene expression, maintenance of genomic stability, cellular senescence regulation, differentiation and development and cellular metabolism. Mice lack the P2 promoter and for other species including pigs the structure of the regulatory elements and expression of isoforms were still unknown. To study the function of the above human p53 isoforms, overexpression or knockout/knockdown experiments were carried out either in cells in vitro or using genetically engineered animal models.

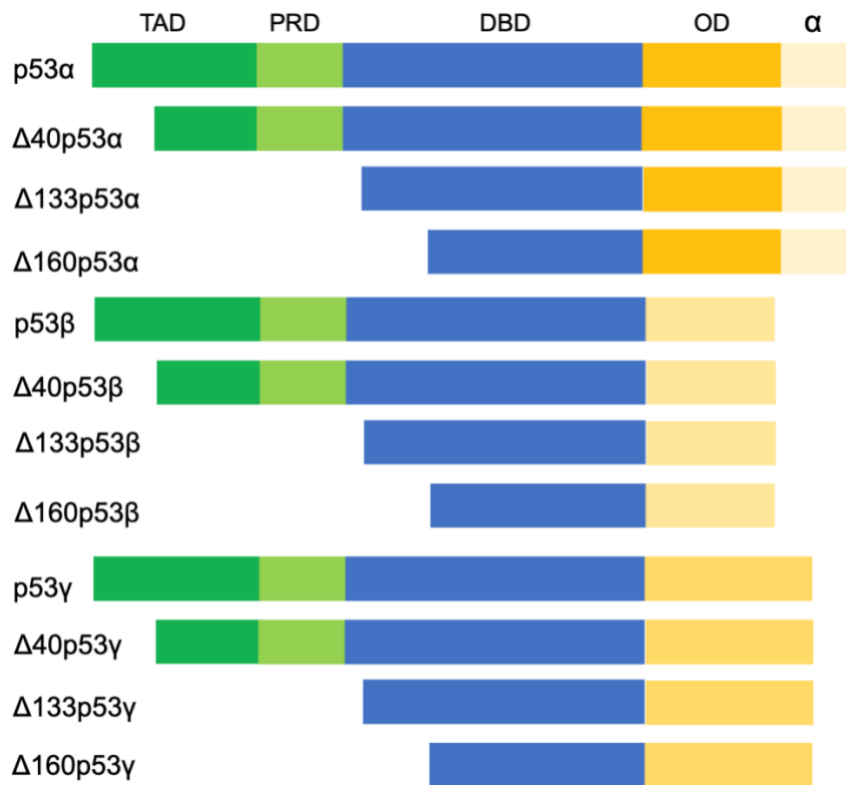


Figure 1.3. *TP53* gene expresses **Isoforms of p53**. Modified from [11]. (TAD: Transactivation domain, PRD: Proline-rich domain, DBD: DNA binding domain, OD: Oligomerization domain)

***TP53* mutated animal models**

The mouse is the most commonly used mammalian species to study gene function. To elucidate *TP53* function, two major categories of mouse models were generated: p53 null mice and mice with specific p53 mutations [12-17]. p53 null mice were generated by several different research groups by disrupting the p53 DNA binding domain [12-14]. In most cases, no embryonic lethality was observed, but the p53^{-/-} mice showed reduced lifespan and developed tumours during the first two months of life, while p53^{+/-} mice developed tumours at a later stage with a median survival of 18 months. Both p53^{-/-} and p53^{+/-} mice developed variety of sarcomas, including osteosarcomas (OS), fibrosarcomas, rhabdomyosarcomas, hemangiosarcomas, leiomyosarcomas, lymphomas, adenocarcinomas and anaplastic sarcomas [12, 13]. Compared to the loss of function, mutations in p53 occur more often in human tumours, in particular at the hotspot sites in the DBD domain (R175, G245, R248, R249, R273, R282) [18, 19]. Several p53 mutant mouse models were generated, which showed enhanced oncogenic ability, e.g. mice expressing the p53 mutants R172H and R270H (orthologous to human R175H and R273H) [20].

Besides mouse, other small animals like rat and zebrafish have been used to investigate the function of p53. A p53 knockout rat was first generated in 2010 by homologous recombination in embryonic stem cells. Later study found out that these rats can develop

lymphomas [21, 22]. In 2011, another model was generated based on the N-ethyl-N-nitrosourea (ENU) method which introduced random point mutations. Complete loss of p53 protein in homozygous rats resulted mainly in sarcomas while heterozygous rats exhibited a delay in tumorigenesis with similar tumour spectrum [23]. In zebrafish, the amino acid sequence is around 48% identical to human p53 [24]. The p53 mutant zebrafish develop a wide tumour spectrum, including malignant peripheral nerve sheath tumours, angiosarcoma, germ cell tumours and leukaemia [25-27].

1.1.2 p63

Like p53, p63 has different isoforms (Figure 1.4). It plays a crucial role in the generation of squamous cell epithelium, contributing to the development of craniofacial structures and the central nervous system. Studies reported the importance of p63 in cell proliferation, differentiation and senescence [28, 29]. p63 is involved in the development of multiple tumours, e.g. breast, lung and prostate tumours [30]. However, unlike p53, p63 is rarely mutated in tumours, and conflicting results were obtained from mouse models. One group detected spontaneous tumours in Trp63+/- mice while another group did not. Nevertheless, its isoform Δ Np63 was considered to promote the tumorigenesis and TAp63 to be a tumour suppressor. But both TAp63 and Δ Np63 isoforms are proven to be suppressors of metastasis [31-33].

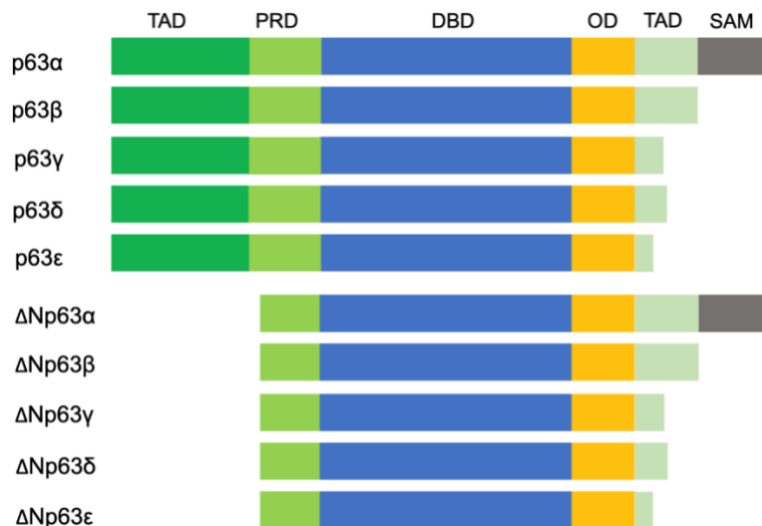


Figure 1.4. Isoforms of p63. Modified from [34] (TAD: Transactivation domain, PRD: Proline-rich domain, DBD: DNA binding domain, OD: Oligomerization domain. SAM: Sterile alpha motif)

1.1.3 p73

p73 was first identified as a homologue of p53, but its function is still not well-understood [35, 36]. In human, p73 has two promoters (P1 and P2), which drive two major isoforms: the full-length TAp73 and N-terminal truncated Δ Np73, which differ by their transactivation function (Figure 1.5) [37, 38]. TAp73 was reported to have a similar function as the tumour suppressor *TP53*, while Δ Np73 acts as an oncogene that has a dominant-negative effect on p53 family members [39]. In contrast to p53, p73 has very low mutation rates (<1%), but it is overexpressed in multiple tumours [40-42], suggesting that both TAp73 and Δ Np73 may play important roles in tumour development. It was confirmed that Δ Np73 is involved in tumorigenesis, but for TAp73, contradiction occurs between its role as tumour suppressor or oncogene. For instance, TAp73 has both negative and positive effects on regulating angiogenesis. Some reports show that TAp73 has tumour suppressive function through the degradation of HIF1- α while others suggest that both isoforms are proangiogenic by supporting cellular survival and tumorigenesis which is also consistent with the overexpression pattern of both isoforms [43-47]. TAp73 is also reported to enhance the pentose phosphate pathway and support oncogenic cell growth [48].

TAp73 is the predominant isoform in SAOS2 cells [49], a human cell line derived from a primary osteosarcoma (OS) and devoid of p53 [50]. One study showed that an overexpression of TAp73 combined with vitamin D could be used as an effective therapeutic strategy against OS [51]. The expression of TAp73 mRNA varies between OS and healthy bone samples; 50% had lower expression in OS than normal tissues, 16.7% had similar and 33.3% even had higher expression in OS [52].

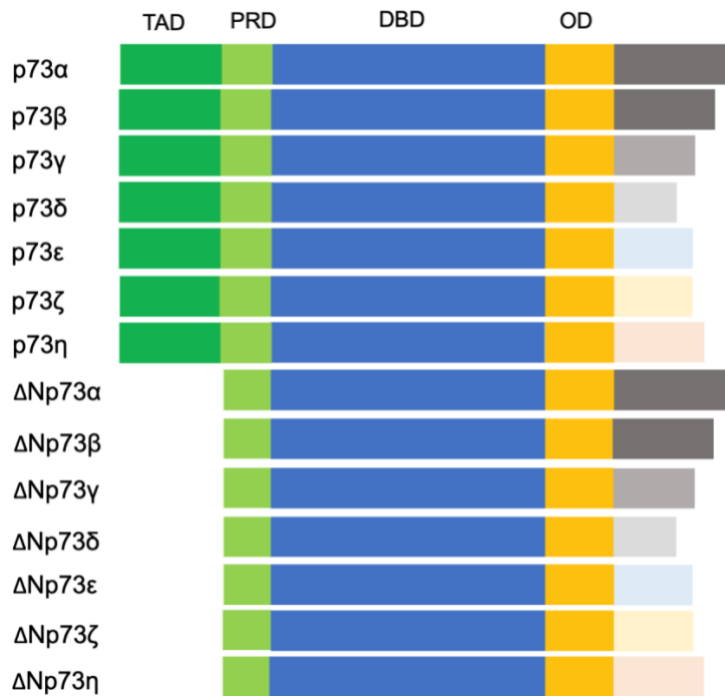


Figure 1.5. The structure of p73 isoforms in human. Modified from [53] (TAD: Transactivation domain, PRD: Proline-rich domain, DBD: DNA binding domain, OD: Oligomerization domain.)

1.2 YAP1 gene

The Hippo pathway was first identified in *Drosophila* and is highly conserved among species [54]. YAP1 (yes-associated protein 1) is a transcriptional coregulator, together with PDZ-binding motif (TAZ), are downstream effectors of hippo signaling pathway in regulating cell proliferation, differentiation, apoptosis and organ size [55]. YAP1 protein can be detected in both the cytoplasm and nucleus of a cell. The phosphorylated YAP1 form is present in the cytoplasm and the dephosphorylated YAP1 is translocated to the nucleus. In the nucleus, YAP1/TAZ complex binds to the transcriptional enhanced associated domain (TEAD) which acts as transcriptional coactivators [56]. Aberrant nuclear localisation of YAP1 was reported in several types of cancers and showed negative correlation with survival rates of patients [57].

Previous studies showed the interaction between the Hippo pathway and p53. YAP1 can bind to the *TP53* promoter and upregulate its expression. Also, the p53 can regulate the expression of *YAP1* [58]. YAP1 and p53 are reported to work together in tumorigenesis. In lung cancer, enhanced nuclear localization and activity of *YAP1* was detected in cells lacking p53 expression and with mutant *KRAS*, which indicated the oncogene property of *YAP1* in the absence of p53 [58]. Other studies reported that YAP1 protein interacted with mutant p53

or $\Delta Np63$ to facilitate oncogenesis [59]. Some research also demonstrated that YAP1 regulated the p73-dependent DNA damaged signaling [60].

1.3 APC gene

First identified in 1991, Adenomatous polyposis coli (*APC*) gene is known as a tumour suppressor, and mutations of *APC* are responsible for the initiation and progression of colorectal cancer [61]. Inherited *APC* mutation leads to multiple adenomatous polyps and familial adenomatous polyposis (FAP) in human colon. Some of these polyps eventually will develop to colorectal cancer in the absence of proper treatment.

Comprising of 15 exons, the *APC* gene encodes a large multi-domain protein (312 kDa, 2843 amino acid and 8529 coding base pairs) and plays an important role in the Wnt signaling pathway [62]. *APC* has 15-amino acid repeats (15AARs) and 20-amino acid repeats (20AARs domains) that bind β -catenin. Other domains can also attract the binding of proteins like Axin, CK1, GSK3 β and EB1 [63]. The *APC* protein is ubiquitously expressed with a high expression in human colon.

APC functions through down-regulating the Wnt signaling pathways by binding and degradation of β -catenin [64]. Loss of *APC* function leads to the hyperactivation of Wnt/ β -catenin signaling pathways by the accumulation of β -catenin in the nucleus which further upregulates the transcription of genes relevant to cell cycle, proliferation, differentiation, and apoptosis [64]. *APC* has also been shown to regulate chromosome segregation and stability by stabilizing microtubules [65].

Germline mutations in the *APC* are responsible for the development of FAP [66]. Patients with germline *APC* mutations are diagnosed with numerous adenomatous polyps. Normally polyps have a combination of germline *APC* mutation and inactivation or mutation of the remaining allele due to somatic mutations or loss of heterozygosity (LOH) at the locus [63]. Previous studies showed that samples with LOH all carried an *APC* mutation around codon 1300. In this context no correlation between LOH and gender, age, or tumour location was observed [67].

1.4 Bone cancer

1.4.1 Osteosarcoma

Osteosarcoma (OS) is the major form of primary bone cancer, prevalent occurring in young people under 20 and adults over 65 (Figure 1.6). For OS patients, aggressive surgical resection and cytotoxic chemotherapy are the most common treatments [68, 69]. Over the past decades, the 5-year survival rate of patients with metastatic OS remained very low, only around 30% [70]. OS often occurs during bone growth, where osteoblastic cells are transformed due to the genetic mutation, such as Li-Fraumeni syndrome, an autosomal dominant genetic disorder caused by germline mutations of p53 [71, 72].

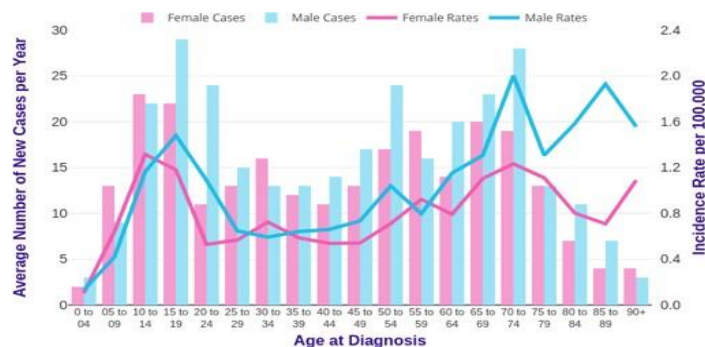


Figure 1.6. Bone sarcoma incidence by age (data from CANCER RESEARCH UK, 2015-2017, UK)

1.4.2 Biology of osteosarcoma

Molecular analysis helped to better understand causes of OS and developed prognosis and treatment strategies. However, genetic contributions to the etiological factors and pathogenesis of OS development still need further investigation.

As with many other tumour types both oncogene activation and tumour suppressor gene inactivation have been observed. For instance, tumour suppressor genes such as *Tp53*, *Rb* (retinoblastoma), *RECQL4*, *BLM* and *WRN* play an important role in OS for patients with Li-Fraumeni, retinoblastoma, Rothmund-Thomson, Bloom or Werner syndromes [73].

1.4.2.1 DNA mutations in osteosarcoma

Using the next generation sequencing, high rate of DNA mutations like somatic point mutations and structural variations were found in OS. Whole exome sequencing revealed around 50000 somatic point mutation and 10000 structural variations were identified in 34 pediatric OS samples [74].

1.4.2.1.1 Chromothripsis and Kataegis in osteosarcoma

Chromothripsis is a mutational process in which ten to thousands of chromosomal rearrangements occur. The chromothripsis has been frequently detected in OS samples [74]. Kataegis is a process of regional hypermutations, which often happen together with chromothripsis. Interestingly, in acute myeloid leukaemia, an association between chromothripsis and somatic p53 mutations has been found [75]. Studies show that telomere

crisis and physical chromosomal damage are the main causes for the induction of chromothripsis in OS [76, 77].

1.4.2.1.2 Cancer driver genes in osteosarcoma

Until now, about 568 driver genes were found to be involved in the process of tumorigenesis, and around 100 in OS [78, 79]. Among them are driver genes like *TP53*, *Rb*, *CDKN2A*, *PTEN* and *YAP1*, which have higher mutations or altered expression in OS. p53 mutations have been discovered in over 60% of the OS patients, indicating its vital role in the carcinogenesis of OS [74, 80, 81]. Rb pathway is revealed to be inactivated in the process of OS, and transgenic mice with inactivated Rb gene develop OS [82, 83]. *CDKN2A* encodes 2 proteins p14 and p16, which are frequently mutated in OS [80, 84]. Downregulation and copy number variations of *PTEN* was detected in over 60% of OS [85]. Furthermore, the importance of *YAP1* on the proliferation of OS cells in mice has been shown [86-88].

1.4.2.2 Epigenetic mechanisms in osteosarcoma

Epigenetics is the study of heritable biological phenomena induced by environmental factors which alter the gene expression by chemical modifications in the chromatin, without the alteration of the DNA sequence. These changes include DNA methylation, acetylation, phosphorylation of histones and other chromatin modifications, nucleosome remodelling [89]. In cancer, these epigenetic modifications mainly happen in oncogenes, tumour suppressors and transcription factors which cause the promotion or inhibition of the gene expression [90]. And these modifications are crucial for the normal development and maintenance of different cell types in mammals. Epigenetic changes are reported to be reversible, which offer the promising possibility for epigenetic therapy by changing the malignant cell status to the normal status [91, 92].

Besides genetic and molecular changes, OS is reported to be induced by the epigenetic changes which block the osteoblastic differentiation of Mesenchymal stem cells (MSCs), these changes include DNA methylation, histone modifications and nucleosome positioning [93].

DNA methylation is an important epigenetic mechanism for altering gene expression by adding a methyl to the cytosine nucleotides that occurs in CpG dinucleotides [94]. The CpG islands of the genes have a low methylation level which ensures the normal expression and altered methylation pattern like hypomethylation and hypermethylation which lead to genomic instability is detected in tumour tissues [95, 96]. Silencing of tumour suppressors by methylation alterations was also detected in OS, research has found that promoter methylation of *Rb* or *p16* can disrupt cell cycle control and thus promote the development of

OS [97]. In the p53 pathway, p53 inactivation was induced by the hypermethylation of the *HIC1* promoter which promotes the OS development [97]. Further data suggested that methylation alteration of the *p14* promoter also induced OS by disrupting the p53 dependent G1 arrest [97]. Moreover, promoter hypermethylation of other tumour suppressor gene like *RASSF1A*, *TIM3*, *FAPK1* was detected in OS cell lines (Figure 1.7) [89].

A histone modification is a covalent post-translational modification (PTM) of the amino termini of the histone proteins which includes methylation, phosphorylation, acetylation, ubiquitylation and sumoylation. Like DNA methylation, it also plays an important role in the regulation of gene expression [98, 99]. Abnormal acetylation and histone modifications are associated with the altered expression of oncogenes and tumour suppressor genes, thus promote to carcinogenesis [100]. Compared to normal cells, histones are hypoacetylated in tumour cells [101]. Histones methylation in position *H3K4*, *H3K36* and *H3K79* are proven to activate the gene transcription, while in *H3K9*, *H3K27* and *H4K20* are related with gene silencing. Therefore, the co-action of histone modifications and DNA methylation plays an essential role.

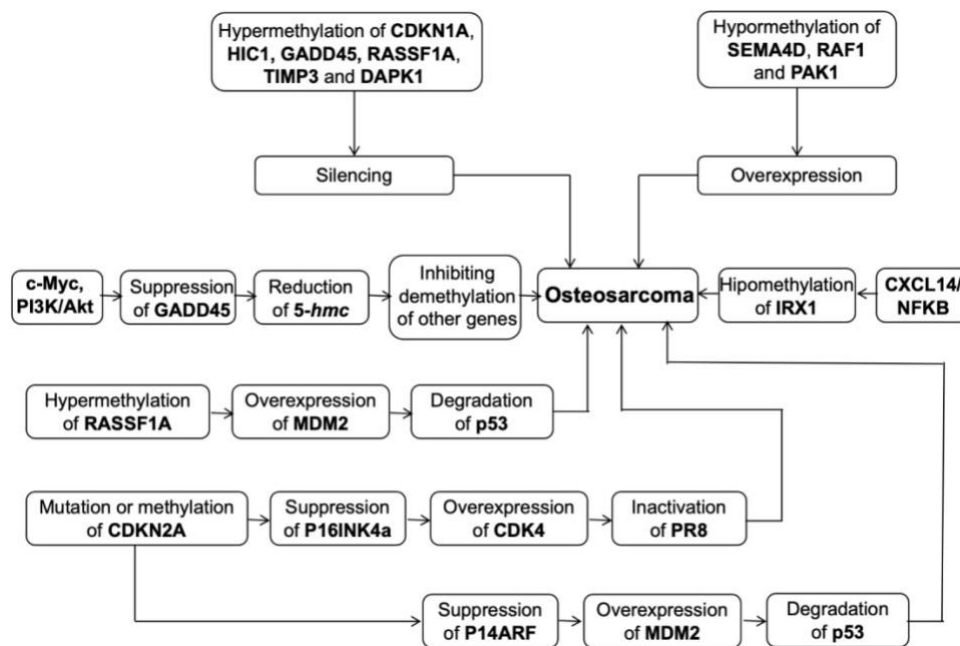


Figure 1.7. Epigenetic events contributing to the initiation and progression of OS.
Modified from [89]

1.4.2.3 Non-coding RNAs in osteosarcoma

Non-coding RNAs play an important role in the regulation of gene function. Non-coding RNAs include miRNAs, long non-coding RNAs (lncRNAs) and circular RNAs (circRNAs). They play a critical role in OS development [102].

miRNAs are demonstrated to be involved in the process of tumorigenesis, e.g. miR-200b has been proven to inhibit the proliferation, migration and invasion of tumour cells including OS via targeting ZEB1 [103], miR-101 functions as a tumour suppressor in OS, overexpression of the miRNA can inhibit the tumour development through the PI3K/AKT and JAK/STAT pathway by inhibiting ROCK1 [104]. Other miRNAs like miR-3928, miRNA-20a, miRNA-19a, miR-574-3p, miR-140, miR-125b, miR-150, miR449c are also reported to regulate the OS development (Figure 1.8) [105-110].

Several lncRNAs have been reported to be involved in the OS development (Figure 1.9), MALAT1 plays a role as an oncogene in OS by targeting RET via activating the PI3K-Akt signal pathway [111]. HOXD-AS1 is reported to aggravate OS oncogenesis by inhibiting the tumour suppressor p57 via interaction with its promoter [112]. Other lncRNAs like SNHG1 and SRA1 are also reported to be involved in OS [113, 114].

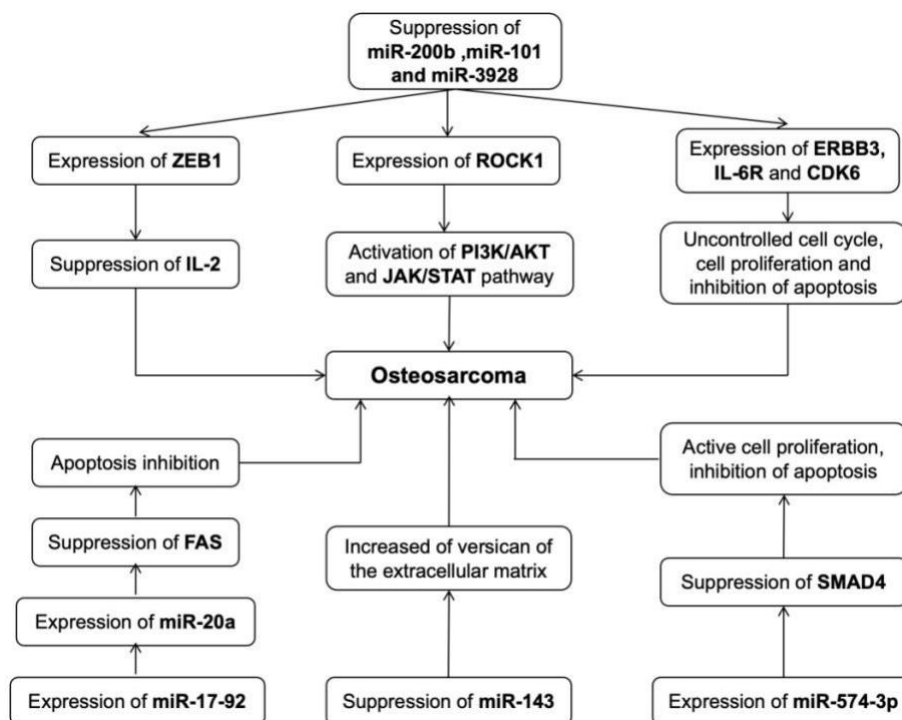


Figure 1.8. Reported miRNAs involved in OS development. Modified from[89]

In OS, circTADA2A is reported to promote OS progression and metastasis, hsa_circRNA_103801 is involved in HIF-1, VEGF and angiogenesis and PI3K-Akt pathway, while hsa_circRNA_104980 in the tight junction pathway (Figure 1.9) [115, 116].

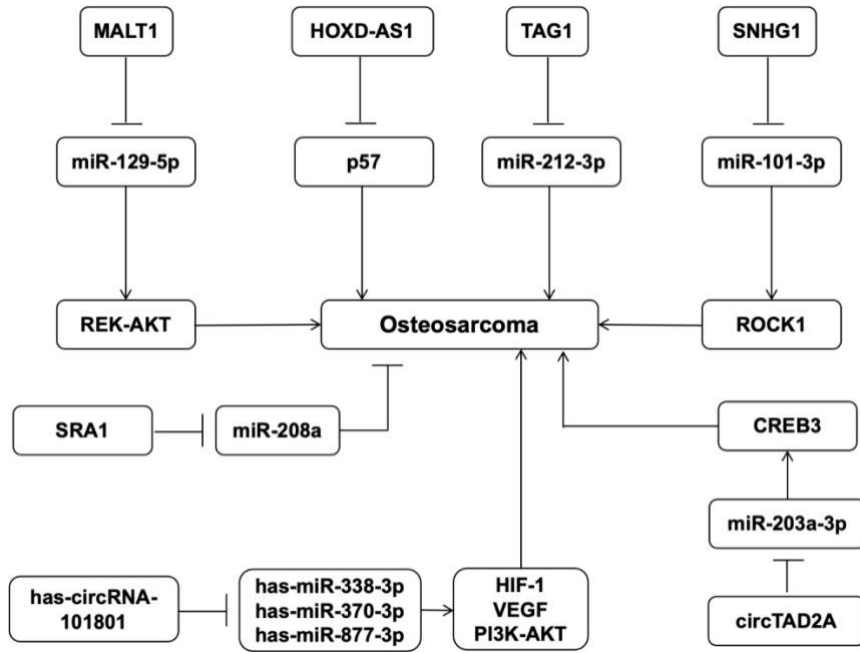


Figure 1.9. Role of lncRNAs and circRNAs in OS. Modified from[89]

1.5 Animal models of osteosarcoma

To better understand the biological basis of OS and to test new therapeutics animal, models are needed. Due to the limited understanding of the aetiology and pathogenesis of OS, it has not been easy to recapitulate the human biology of OS in animal models.

Therefore, there is no single animal model of OS to fully characterize the biological and clinical features. Studies of OS models mainly focus on mouse, rat, dog and pig [117].

1.5.1 Canine model of osteosarcoma

Spontaneous OS is more often diagnosed in large and giant dogs than in humans [117]. Dogs share the same environment as human, which provides dogs with big advantages compared to mice to study OS [118]. Interestingly, OS shows similar gene expression pattern between humans and dogs. Mutations in genes like *PTEN*, *Rb* and *p53* are frequently detected in the canine OS [119]. Some dog breeds may carry germline mutations like human Li-Fraumeni syndrome contributing to a higher risk of cancer.

1.5.2 Mouse model of osteosarcoma

While the canine model provides a good option to study human OS, spontaneous OS in dogs can have various causes which complicate the analysis. A representative and controllable OS animal model with defined mutations is a better way to understand OS. Many mouse models of OS have been developed by targeting some important tumour suppressor genes like *p53* and *Rb* [120, 121]. The *p53* knockout mice developed OS in around 4% of homozygous and 20% of heterozygous animals [13, 14]. The low ratio of tumour in

homozygous knockout mice might be caused by the high death rates induced by blood cancer in p53 null mice. P53 mutant knock-in mice were developed with R172H (orthologs to human R175H mutation) or other mutations, these mice can not only develop OS but also show metastasis to other organs [20]. Some other mouse models of OS were developed such as c-fos, p14, p16 and p21, providing a better understanding of OS [122-125].

1.5.3 Rat model of osteosarcoma

A rat model of OS was first reported in 1970 by the radiation of ³²P-impregnated sheets of polyvinyl chloride (PVC), and the incidence of OS after 18 months was 28% [126]. Another OS rat model produced by the intrafemoral injection of human OS cells in Sprague-Dawley rats developed OS in 80% of animals at the injection site and 96% of the animals had lung metastasis [127]. In 2009, a new OS rat model was established by orthotopic implantation, tumour expanded vigorously in the first three weeks [128].

1.5.4 Pig model of osteosarcoma

Compared to mouse models, pig models share higher similarities with human, like body size, anatomical features and pathophysiology. To date, two pig OS lines have been reported. Sieren et al. have generated Yucatan minipigs that carry a R167H mutation in the endogenous *TP53* gene that is ubiquitously expressed [129]. Heterozygous *TP53*^{R167H} pigs developed no tumours even at the age of 30 months, while homozygous animals developed a variety of tumours, including osteogenic tumours, lymphomas and renal tumours when they reached sexual maturity, broadly recapitulating the tumour spectrum observed in human and mice with the orthologous mutation [129].

In the Chair of Livestock Biotechnology pigs carrying a latent *TP53*^{167H} mutation in exon 5 that can be activated by Cre-mediated excision of an upstream transcriptional stop signal were generated [130, 131]. The major *TP53* transcript is blocked by a stop signal in its uninduced form [130, 131]. The heterozygous pigs develop OS after 16 months of age, while homozygous pigs show OS at 7-8 months. Wilm's tumours and lymphomas also occur occasionally [130, 131]. The sarcomas primarily affect the long bones, skull and mandible, which is similar to human [121, 131]. Porcine OS cells show similar cytogenetic abnormalities as in humans, like abnormal giant nuclei, micronuclei and multinuclear cells with fragmented nuclei and atypical mitotic processes [131]. In human, tumour cells show abnormal karyotype and increased resistance to radiation [131]. The differences between the pathological phenotypes exhibited by these two pig lines provide valuable resources to further analysis the underlying mechanisms that initiate this fatal disease. They also offer the possibility to identify possible drugs and surgical treatments for this disease.

1.6 Colorectal cancer

Colorectal cancer (CRC) is one of the most common cancer types around the world, causing around 800,000 deaths per year among both sexes [132]. The decline in incidence and mortality over the past years can be attributed to improvements in early detection and effective therapeutic interventions for the late-stage CRC [132]. CRC development process is initiated by transformation of normal epithelium cells of the colon wall leading to adenomatous polyps.

1.6.1 Biology of colorectal cancer

The genetic process of CRC is complicated and heterogeneous, including somatic and germline gene mutations, epigenetic changes, noncoding RNA regulation, point mutation, gene bases insertion or deletion. Over 80% CRC arise sporadically while less than 20% is inherited [133]. Sporadic CRC occurs mainly in old age and there is no genetic family history, while inherited CRC patients have a family history of CRC. The inherited CRC patients have penetrant cancer syndromes, like Familial adenomatous polyposis (FAP) [133]. Since the association of *APC* and FAP, the regulation of *APC* contributing to CRC has been further studied. FAP is a rare genetic colorectal cancer predisposition syndrome that can developed into classic or attenuated form. For patients with classic form of FAP, 95% of them have polyps by the age of 35 years. The average age of CRC diagnosis in untreated condition is 39 years. Those with attenuated form have an ca. 70% lifetime risk of CRC and average diagnosis age of around 50 to 55 years.

FAP is caused by germline mutations in the *APC* gene and is inherited in an autosomal dominant manner, meaning that an average of 50% of the children of the affected parents will have inherited the disease [134].

Our group developed a porcine model of Familial Adenomatous Polyposis that carries a premature translational stop signal at the codon 1311 in the *APC* gene, which is orthologous to human *APC*¹³⁰⁹ mutation [135]. *APC*^{1311/+} pigs have more than one hundred of macroscopically visible lesions which including over 60 sessile polyps in the colon and rectum at 1 year age [135]. These data showed that in pigs, *APC* mutations result in polyposis in large intestine as human, unlike mice in small intestine.

1.6.1.1 Epigenetic regulation in colorectal cancer

Methylation analysis of the CpG island of *APC* has been studied by several groups. Manel Esteller *et al.* revealed that aberrant *APC* methylation was detected early in colorectal carcinogenesis. The *APC* promoter was hypermethylated in 18% of primary sporadic CRC, and neoplasia. Hypermethylation blocks *APC* transcription and impairs its tumour suppressor

function [136]. Bing-Qiang Li *et al.* found that methylation of *APC* was correlated with tumour size, differentiation degree as well as lymph node metastasis of patients [137]. While Alan Aitchison *et al.* reported that methylation of *APC* promoter was detected in 40% of CRC and there was no correlation between methylation and age, gender or tumour location [67].

1.6.1.2 Non-coding RNA in colorectal cancer

MiRNAs are widely involved in the progression of CRC. For example, miR-143 and miR-145 were downregulated in CRC [138]. Overexpression miR-124 was shown to inhibit the CRC proliferation and induce cell cycle arrest [139]. In the *APC*^{1311/+} pigs, miR-17-5p was found to regulate the *APC* expression [140]. Other miRNAs such as miR-200 and miR-139 were involved in the pathogenesis of CRC [141, 142].

Several long non-coding RNAs (lncRNAs) are associated with CRC. For example, *HOTAIR* is promoting CRC and its knockdown inhibited migration, invasion, and proliferation of CRC cells [143]. lncRNA *RAMS11* was upregulated in CRC and promoted the tumour growth and metastasis, downregulation of *RAMS11* was found to inhibit the proliferation and metastasis of CRC cells [144]. Other lncRNAs like *FLNC* and *H19* were also reported to modulate the CRC progression [145, 146].

Compared to miRNA and lncRNA involvement and understanding of circRNA is still in its infancy in CRC research. Circ002144 was upregulated in CRC and associated with cell invasion, proliferation and migration [147]. Abnormally expression of circ002144 was correlated with prognosis which indicated that circ002144 might be a biomarker for the evaluation of CRC [147]. ciRS-7 was proved to be promote the CRC through the repression of miR-7 [148]. CircRNA *FBXW7* was reported to inhibit proliferation, migration and invasion of CRC cells which showed the diverse role of circRNAs in the modulation of CRC [149].

1.7 Animal model of colorectal cancer

1.7.1 Mouse model of colorectal cancer

Carcinogen induced mice were first developed for CRC model with chemicals and radioactive elements. These CRC models were widely applied in the study of relations between CRC risk and dietary, gut microbiome as well as radioactive treatment [150, 151]. However, the carcinomas barely showed an invasive and metastatic disease.

The first genetically engineered mouse model of CRC was the *Apc*^{min} mouse with mutated *APC* codon 380 [152]. These mice developed adenomas in the small intestine which promoted the study of early stages of FAP, but failed to mimic most spontaneous CRC [153]. Other *APC* mutant mice models including *APC*^{Δ14/+}, *APC*^{Δ242/+}, *APC*^{+/-Δ716} were generated

[154-156]. To accelerate the disease progression *APC* mutant mice were crossed with mutant *Tp53*, *Kras* mice [157-160].

Some other transgenic mice targeting other genes than *APC* also developed colorectal tumour and metastasis [161].

1.7.2 Rat model of colorectal cancer

Like mouse model, the early-stage rat model of CRC was induced by chemicals like radioactive yttrium, cycad flour and azoxymethane (AOM). Transgenic Rat like F344-Pirc was derived with a knockout allele of *APC* gene [162]. These rats developed similar adenomas as human in the carcinomas progression and gender dependent variation [162]. The Kyoto *Apc* Delta (KAD) rat was generated with ENU mutations and one *APC* mutation at codon 2523, these rats didn't develop tumours spontaneously, and AOM treatment induced intestinal neoplasia [163, 164].

1.7.3 Pig model of colorectal cancer

Our group developed a genetically modified pig with endogenous *APC* 1311 mutation which is orthologous to human *APC* 1309 [135]. Similar to human patients, the number of polyps can vary between siblings with the same *APC* mutation. However, the genetic determinant for this is unknown [135].

1.8 Aim of the thesis

An important question in cancer biology is that why do specific mutations induce carcinogenesis in a limited number of tissues. Oncopigs with a whole body inactivation of *TP53* showed a limited tumour spectrum in both hetero- and homozygous animals which all developed OS. Therefore the first 2 two aims of the thesis were to 1. identify the genetic determinant of high OS frequency in the *TP53* mutant pigs. 2. define modifying genes responsible for maintaining OS.

A second oncopig line, the *APC* 1311 line to model colorectal cancer, develops polyposis at an early age (3 month). However, the number of polyps varies greatly between siblings. This has also been observed in human FAP patients, but the molecular basis for the disease severity has so far not been identified. Therefore, the third aim of the doctoral thesis was to investigate the molecular mechanisms contributing to the severity of FAP in the *APC*^{1311/+} pigs.

2. Materials and Methods

2.1 Materials

2.1.1 Lab equipment

Table 2.1 Lab equipment

Equipment	Company
+4°C fridge	Beko Technologies, Dresden, GER
-20°C freezer	Siemens, Munich, GER
-80°C freezer	Thermo Electron GmbH, Dreieich, GER
2100 Bioanalyzer	Agilent, Santa Clara, USA
3130xl/3100 Genetic Analyzer 16-Capillary Array	Life Technologies, Darmstadt, GER
ABI 7500 Fast Real-Time PCR System	Applied Biosystems, Warrington, GBR
ABI Prism 3130xl Genetic Analyzer	Life Technologies, Darmstadt, GER
Analytical semi-micro balance PI-214	Denver Instrument GmbH, Göttingen, GER
Axiovert 200 M	Carl Zeiss Microscopy GmbH, Göttingen, GER
Bag sealer Vacupack plus	KRUPS, Frankfurt, GER
Barnstead MicroPure	Thermo Fisher Scientific, Waltham, USA
Centrifuges Sigma 1-15, 1-15K, 3-16 and 4K-15C	Sigma-Aldrich Chemie GmbH, Steinheim, GER
Countess™ automated cell counter	Invitrogen GmbH, Darmstadt, GER
Digital Graphic Printer UP-D895MD	Syngene, Cambridge, GBR
Dry block for heating and cooling PCH-2	Grant Instruments, Cambridge, GBR
Drying and heating chamber	BINDER GmbH, Tuttlingen, GER
Electronic multi-dispense pipet	Qiagen, Hilden, GER
Electrophoresis power supply EPS301	Amersham Biosciences, Piscataway, USA
Fluorescence light source HXP120C	Carl Zeiss Microscopy GmbH, Göttingen, GER
Gel documentation system QUANTUM ST5	VILBER LOURMAT Deutschland GmbH, Eberhardzell, GER
Glassware	Marienfeld GmbH, Lauda-Königshofen, GER
HiSeq 2500	Illumina, San Diego, USA
Hybridisation oven Shake'n'Stack	Thermo Fisher Scientific, Waltham, USA
iBind Western Device	Thermo Fisher Scientific, Waltham, USA
Ice maker	Manitowoc Company Inc., Manitowoc, USA
Incubator Thermo Forma Orbital Shaker	Thermo Fisher Scientific, Waltham, USA
Incubator Thermo Forma Steri-Cycle CO2	Thermo Fisher Scientific, Waltham, USA
Laser Microdissection Systems 6000	Leica Microsystems, Wetzlar, GER

Liquid nitrogen tank	KGW-Isotherm Karlsruher Glastechnisches Werk - Schieder GmbH, Karlsruhe, GER
Mi Seq	Illumina, San Diego, USA
Microm HM 560 Cryostat	Thermo Fisher Scientific, Waltham, USA
Microscope Axiovert 40 CFL	Carl Zeiss Microscopy GmbH, Göttingen, GER
Mini-PROTEAN 3 Cell system	BioRad, Hercules, USA
Mini-PROTEAN® Comb, 10-well, 0.75 mm, 33 µl, 1653354 and 1.5 mm, 66 µl, 1653365	BioRad, Hercules, USA
Mini-PROTEAN® Short Plates, 1653308	BioRad, Hercules, USA
Mini-PROTEAN® Spacer Plates with Integrated Spacers 1.5 mm, 1653312	BioRad, Hercules, USA
Multiporator Eppendorf	Eppendorf, Hamburg, GER
Nalgene™ Mr. Frosty Freezing containers	Thermo Fisher Scientific, Waltham, USA
Nanodrop Lite	Thermo Fisher Scientific, Waltham, USA
Nucleofector™ 2b Device	Lonza Group Ltd, Basel, CHE
Owl™ EC-105 Compact Power Supply	Thermo Fisher Scientific, Waltham, USA
PeqSTAR 2x Gradient Thermocycler	Peqlab Biotechnologie GmbH, Erlangen,GER
pH Meter CyberScan PC 510 Meter	Eutech Instruments Europe B.V., Landsmeer, NLD
Pipette controller accu-jet pro	Brand GmbH & Co. KG, Wertheim,GER
PyroMark Q48 Autoprep Instrument	Qiagen, Hilden, GER
Qubit® 2.0 Fluorometer	Thermo Fisher Scientific, Waltham, USA
Rainin Pipet-Lite (2, 20, 200, 1000 µl) and Multi Pipette L8-20XLS+, L8-50XLS+	Mettler Toledo GmbH, Giessen, GER
Scales 440-33N	Kern & Sohn GmbH, Balingen, GER
Shaker Unitwist 3-D	Uniequip, Martinsried,GER
SpeedMill PLUS	Analytik Jena AG, Jena, GER
Sterile laminal flow cabinet Herasafe Type HSP	Thermo Fisher Scientific, Waltham, USA
Table centrifuge blue spin mini	SERVA Electrophoresis GmbH, Heidelberg, GER
Trans-Blot SD Semi-Dry Transfer cell	BioRad, Hercules, USA
Vacuum Centrifuge Savant, SpeedVac, DNA 110	Thermo Fisher Scientific, Waltham, USA
Vacuum Centrifuge Savant, Speed Vac Plus, SC110A	Thermo Fisher Scientific, Waltham, USA
Vortexer VELP Sccientifica 2x3	Velp Scientifica, Usmate, ITA
Water bath	Memmert GmbH + Co.KG, Schwabach, GER
X-ray clip cassette	Rego X-Ray GmbH, Augsburg,GER

2.1.2 Consumables

Table 2.2 Consumables

Product	Company
0.5, 1.5, 2.0 ml reaction tubes	Brand GmbH & Co. KG, Wertheim, GER
1.0, 2.0, 5.0, 10.0, 25.0 ml disposable serological pipettes	Corning Inc., New York, USA
14ml round-bottom tubes	BD, Baltimore, USA
15ml and 50ml conical bottom centrifugation tubes	Greiner Bio-One GmbH, Frickenhausen, GER
Disposable pipet tips	Brand GmbH & Co. KG, Wertheim, GER
Blotting Paper	BioRad, Hercules, USA
Cell counting chamber slides	Invitrogen GmbH, Darmstadt, GER
Cell scraper	Faust Lab Science, Klettgau, GER
Countess™ cell counting chamber slides	Invitrogen GmbH, Darmstadt, GER
Cryo Tube vials	Corning Incorporated, Corning, USA
Cutfix stainless scalpel 10	B. Braun Melsungen AG, Melsungen, GER
Disposable sterile needles, Sterican, 1.20 x 40 mm	B. Braun Melsungen AG, Melsungen, GER
Electroporation cuvette 2, 4 mm	Peqlab Biotechnologie GmbH, Erlangen, GER
Falcon tubes 15 ml, 50 ml	Greiner Bio-One GmbH, Frickenhausen, GER
iBind cards, Bi15126	Invitrogen GmbH, Darmstadt, GER
innuSPEED Lysis Tube P	Analytik Jena AG, Jena, GER
Kimtech Science Precision wipes, 05511 7552	Kimberly-Clark Professional, Roswell, USA
Lysing Matrix D, 2 ml Tube	MP Biomedicals, Santa Ana, USA
Membrane, Roti-PVDF (0.45 µm)	Brand GmbH & Co. KG, Wertheim, GER
MembraneSlide 1.0 PEN (D), 415190-9041-000	Carl Zeiss Microscopy GmbH, Göttingen, GER
MicroAmp™ Optical Adhesive Film, 4360954	Applied Biosystems, Warrington, GBR
Mini Trans-Blot Filter paper, 1703932	BioRad, Hercules, USA
MultiScreen HV plates, MAHVN4550	Millipore, Darmstadt, GER
Nylon membrane (positively charged)	GE Healthcare Europe GmbH, Freiburg, GER
PCR tube 0.2 ml 8- strip, I1402-2900	STARLAB International GmbH, Hamburg, GER
Petri dishes	Brand GmbH & Co. KG, Wertheim, GER
Rainin pipette tips with filter 20, 200, 1000 µl	Mettler Toledo GmbH, Giessen, GER
Reaction tubes 1.5 ml, 2 ml	Zefa Laborservice, Harthausen, GER
Serological pipets Costar 1, 2, 5, 10, 25 ml	Corning Incorporated, Corning, USA
Sterile syringes 5 ml, 10 ml, 20 ml	Becton Dickinson GmbH, Sparks, USA
Sterile syringe filters 0.40 µm, 0.22 µm	Berrytec GmbH, Grünwald, GER

Tissue culture vessels T25, T75, T150,	Corning Incorporated, Corning, USA
24 ,12, 6 well plates, 10 and 15 cm dishes	
Tissue-Tek Cryomold® Biopsy, 4565	Sakura Finetek Europe
PCR Plate 96 semi skirted, colorless, 951020303	Eppendorf, Hamburg, GER
PyroMark Q48 Absorber Strips, 974912	Qiagen, Hilden, DEU
PyroMark Q48 Discs, 974901	Qiagen, Hilden, DEU
X-ray film	Agfa Healthcare, Mortsel, Belgium

2.1.3 Chemicals

Table 2.3 Chemicals

Product	Company
Acetic acid	Applichem, Darmstadt, GER
Agarose	Sigma-Aldrich Chemie GmbH, Steinheim, GER
Ammonium persulfate (APS)	Carl Roth GmbH, Karlsruhe, GER
Ampicillin	Sigma-Aldrich GmbH, Steinheim, GER
Boric acid	AppliCHEM GmbH, Darmstadt, GER
Chloroform	Applichem, Darmstadt, GER
Crystal violet	Sigma-Aldrich GmbH, Steinheim, GER
DAPI	Roche Diagnostic GmbH, Mannheim, GER
DMSO	Applichem, Darmstadt, GER
Dithiothreitol (DTT)	Omnilab, Bremen, GER
Eosin solution, Conc. Watery 2 %, 2C-140	Waldeck GmbH & Co. KG, Münster, GER
Ethanol absolute	Riedel-de-Haen, Seelze, GER
Ethidium bromide	Sigma-Aldrich GmbH, Steinheim, GER
Ethylenediaminetetraacetic acid	AppliCHEM GmbH, Darmstadt, GER
Formalin	Sigma-Aldrich Chemie GmbH, Steinheim, GER
Glucose	Sigma-Aldrich GmbH, Steinheim, GER
Glycine	Carl Roth GmbH, Karlsruhe, GER
Glycerol 99%	AppliCHEM GmbH, Darmstadt, GER
Hydrochloric acid, 37%	Sigma-Aldrich Chemie GmbH, Steinheim, GER
IGEPAL, CA-630	Sigma-Aldrich Chemie GmbH, Steinheim, GER
Isopropanol	Applichem, Darmstadt, GER
IPTG	Bioline, London, GBR
Maleic acid	Sigma-Aldrich Chemie GmbH, Steinheim, GER
Mayer's Hemalaun solution	Applichem, Darmstadt, GER
Methanol	Sigma-Aldrich Chemie GmbH, Steinheim, GER

MgCl ₂	Merck, Kenilworth, USA
Milk powder	Carl Roth GmbH, Karlsruhe, GER
N, N-Dimethylformamide (DMF)	Sigma-Aldrich Chemie GmbH, Steinheim, GER
Nonidet P-40	Sigma-Aldrich GmbH, Steinheim, GER
Phenol-chloroform-isoamyl alcohol	pplichem, Darmstadt,GER
Sodium chloride	Applichem, Darmstadt,GER
Sodium dodecyl sulphate (SDS)	Omnilab, Bremen, GER
Sodium hydroxide (NaOH)	Sigma-Aldrich Chemie GmbH, Steinheim, GER
Sodium chloride	Applichem, Darmstadt,GER
Sodium citrate	Sigma-Aldrich Chemie GmbH, Steinheim, GER
Spectinomycin	Fluka Laborchemikalien GmbH, Seelze, GER
Tetramethyl ethylenediamine (TEMED)	Carl Roth GmbH, Karlsruhe, GER
Triton-X 100	Omnilab, Bremen,GER
Trizol	Invitrogen GmbH, Darmstadt, GER
Tween 20	Sigma-Aldrich Chemie GmbH, Steinheim, GER
X-ray tank developer	Calbe Chemie GmbH, Calbe,GER
X-ray tank fixer	Calbe Chemie GmbH, Calbe, GER
β-glycerol phosphate	Sigma-Aldrich Chemie GmbH, Steinheim, GER
β-mercaptoethanol (14.3 M)	Sigma-Aldrich Chemie GmbH, Steinheim, GER

2.1.4 Buffer and Solution

Table 2.4 Buffer and Solution

1x Semi Dry Transfer Buffer + 0.1% SDS	25 mM Trizma Base, 0.2 M Glycin, 20 % (v/v) Methanol, 0.1 % (w/v) SDS
1x TBST	20 mM Trizma Base, 140 mM NaCl, 0.1 % (v/v) Tween 20
1x WB Running Buffer + β-mercapto-Ethanol	25 mM Trizma Base, 0.2 M Glycin, 0.1 % SDS, pH 8.3, 10.64 mM β-mercaptoethanol
2 log DNA ladder	New England Biolabs, Frankfurt, GER
4 x Lämmli buffer + DTT	250 M Tris-HCl, pH 6,8, 4 % (w/v) SDS, 0,1 M Saccharose, traces of bromophenol blue, 26mM DTT (freshly added)
5x dilution buffer	25 mM MgCl ₂ , 1 mM Tris-HCl pH 8.0
6x Gel loading dye	New England Biolabs, Frankfurt, GER
10x TBE buffer	0.9 M Tris, 20 mM EDTA, 0.9 M boric acid
10x TBS	0.2 M Trizma Base, 1.4 M NaCl
10x WB Running Buffer, pH 8.3	0.25 M Trizma Base, 2 M Glycin, 1 % SDS, pH 8.3
10 % APS	10 % (w/v) APS

50x TAE buffer	2 M Trisbase, 50 mM EDTA, 5.71 % (v/v) Glacial acetic acid
Advanced protein assay reagent	Cytoskeleton Inc., Denver, USA
Anti-Digoxigenin-AP Fab fragment	Roche Diagnostic GmbH, Mannheim, GER
cOmplete Protease Inhibitor Cocktail Tablets in EASYpacks	Roche Diagnostic GmbH, Mannheim, GER
CytoBuster™ Protein Extraction Reagent, 71009	Merck, Kenilworth, USA
DNA/RNA-dye, peqGREEN	Peqlab Biotechnologie GmbH, Erlangen, GER
dNTPs	New England Biolabs, Frankfurt, GER
EB Buffer	Qiagen, Hilden, GER
LB-agar	4 % (w/v) Difco LB Agar, Miller
LB-medium	2.5 % (w/v) Difco LB Base, Miller
Lysis buffer for gDNA isolation	100 mM Tris-HCl pH7.4, 0.2 % SDS, 5 mM EDTA, 0.2 M NaCl
Matrigel™ Basement Membrane Matrix, high concentrated	BD, Baltimore, USA
Milk powder blocking solution	5 % (w/v) Milk powder in 1x TBST
β-mercaptoethanol solution for TC	6 ml H ₂ O, 21 μl β-mercaptoethanol
O.C.T.™ Compound, 4583	Sakura Finetek Europe B.V., Alphen aan den Rijn, NLD
PhosSTOP Phosphatase Inhibitor Cocktail Tablets in EASYpacks, 04906845001	Roche Diagnostic GmbH, Mannheim, GER
Pierce™ ECL Western Blotting substrate	Thermo Scientific, Waltham, USA
PyroMark Q48 Magnetic Beads, 974203	Qiagen, Hilden, GER
Rnase Away	Thermo Fisher Scientific, Waltham, USA
Spectra™ Broad Range Protein Ladder	Fermentas GmbH, St. Leon-Rot, GER
TE Buffer	10 mM Tris-HCl pH 7.4, 1 mM EDTA
Trypan blue solution	Sigma-Aldrich Chemie GmbH, Steinheim, GER
Tryptone	Fluka, Seelze, GER
X-Gal solution	100 mg X-Gal in N, N-Dimethylformamid (DMF)
Yeast extract	Fluka, Seelze, GER

2.1.5 Tissue culture media and buffer

Table 2.5 Tissue culture media and buffer

Product	Company
1x Trypsin EDTA, T3924	Sigma-Aldrich Chemie GmbH, Steinheim,

	GER
Accutase, A6964	Sigma-Aldrich Chemie GmbH, Steinheim, GER
Advanced DMEM, 12491-015 1	Life Technologies, Darmstadt, GER
Amphotericin B solution, A2942	Sigma-Aldrich Chemie GmbH, Steinheim, GER
Blasticidin S	Sigma-Aldrich Chemie GmbH, Steinheim, GER
BSA 7.5 %	Life Technologies, Darmstadt, GER
cell culture water, W3500	Sigma-Aldrich Chemie GmbH, Steinheim, GER
DMEM	Sigma-Aldrich Chemie GmbH, Steinheim, GER
DPBS	Sigma-Aldrich Chemie GmbH, Steinheim, GER
Fetal calf serum	Biochrom GmbH, Berlin, GER
G-418, M3118.0050	Genaxxon bioscience GmbH, Ulm, GER
Hygromycin	InvivoGen, San Diego, USA
Hypoosmolar electroporation buffer	Eppendorf, Hamburg, GER
Non-essential amino acids (NeAA), M7145	Sigma-Aldrich Chemie GmbH, Steinheim, GER
OptiMEM, 51985-026	Life Technologies, Darmstadt, GER
Penicillin-Streptomycin, P0781 (100x)	Sigma-Aldrich Chemie GmbH, Steinheim, GER
Puromycin	InvivoGen, San Diego, USA
Sodium pyruvate, S8636	Sigma-Aldrich Chemie GmbH, Steinheim, GER
Trypan blue 0.4 %	Invitrogen GmbH, Darmstadt, GER

2.1.6 Kits

Table 2.6 Kits

Product	Company
Agilent RNA 6000 Nano Kit	Agilent, Santa Clara, USA
Agilent RNA 6000 Pico Kit	Agilent, Santa Clara, USA
AllPrep DNA/RNA Mini Kit	Qiagen, Hilden, GER
CloneJET PCR Cloning Kit	Thermo Fisher Scientific, Waltham, USA

exoRNeasy Serum/Plasma Maxi Kit	Qiagen, Hilden,GER
EZ DNA Methylation-Direct™ Kit	Zymo Research, Tustin, USA
EZ RNA Methylation-Direct™ Kit	Zymo Research, Tustin, USA
Fast SYBR™ Green Master Mix	Applied Biosystems, Warrington, GBR
FirstChoice™ RLM-RACE Kit	Invitrogen GmbH, Darmstadt, GER
GenElute Mammalian Genomic DNA Purification Kit	Sigma-Aldrich Chemie GmbH, Steinheim,GER
HiSeq Rapid PE Cluster Kit v2	Illumina, San Diego, USA
HiSeq Rapid SBS Kit v2 (200 cycles), FC-402-4021	Illumina, San Diego, USA
iBind™ Solution Kit	Invitrogen GmbH, Darmstadt, GER
innuPREP RNA Mini Kit	Analytik Jena AG, Jena,GER
KAPA SYBR FAST Master Mix Universal 2X	Kapa Biosystems, Wilmington, USA
Lipofectamine™ 2000 Transfection Reagent	Invitrogen GmbH, Darmstadt, GER
Lipofectamine™ 3000 Transfection Reagent	Invitrogen GmbH, Darmstadt, GER
pGEM®-T Easy Vector System	Promega Corporation, Madison, USA
Plasmid DNA purification NucleoBond® Xtra Midi	MACHEREY-NAGEL GmbH, GER
PyroMark Q48 Advanced CpG Reagents	Qiagen, Hilden,GER
TruSeq RNA Library Preparation Kit v2, Set A	Illumina, San Diego, USA
TURBO DNA-free™ Kit	Invitrogen GmbH, Darmstadt,GER
Wizard® SV Gel and PCR Clean-Up System	Promega Corporation, Madison, USA

2.1.7 Enzymes

Table 2.7 Enzymes

product	Company
AccuStart Taq DNA Polymerase HiFi	Quantabio, Beverly, USA
Collagenase Type I-A, C2674	Sigma-Aldrich Chemie GmbH, Steinheim, GER
DNA Polymerase I, Large Klenow Fragment	New England Biolabs, Frankfurt,GER
FastGene® Optima HotStart ReadyMix	NIPPON Genetics Europe, Dueren, GER
PCR Extender System	5Prime GmbH, Hamburg,GER
Proteinase K	Sigma-Aldrich Chemie GmbH, Steinheim, GER
PyroMark PCR Kit	Qiagen, Hilden,GER
Q5® High-Fidelity DNA Polymerase	New England Biolabs, Frankfurt, GER
Quickextract	Epicentre, Madison, USA
Restriction enzymes	New England Biolabs, Frankfurt, GER
RiboLock Rnase Inhibitor, EO0381	Thermo Fisher Scientific, Waltham, USA

RNase A	Sigma-Aldrich Chemie GmbH, Steinheim, GER
Shrimp alkaline phosphatase	New England Biolabs, Frankfurt, GER
Sssl, CpG methyl transferase	New England Biolabs, Frankfurt, GER
SuperScript TM II, III and IV Reverse Transcriptase	Invitrogen GmbH, Darmstadt, GER
T4 DNA Ligase	New England Biolabs, Frankfurt, GER

2.1.8 Antibodies

Table 2.8 Antibodies

name	source
moues monoclonal anti-GAPDH #G8795	Sigma-Aldrich Chemie GmbH, Steinheim, GER
rabbit anti-mouse IgG H&L (HRP) ab6728	Abcam, Cambridge, England
polyclonal rabbit anti-YAP1 ARP50530	Aviva Systems Biology Corporation, USA
HRP labelled anti-rabbit sc-2004	Santa Cruz Biotechnology, USA
sheep Sapu antibody	gift from University of Dundee, GBR
horseradish peroxidase (HRP) labelled anti-sheep s36-62DD	Invitrogen GmbH, Darmstadt, GER
rabbit anti-p63 monoclonal antibody ab124762	Abcam, Cambridge, England
rabbit anti-p73 polyclonal antibody PA5-80175	Invitrogen GmbH, Darmstadt, GER
rabbit anti-MDM2 polyclonal antibody ab260074	Abcam, Cambridge, England
Goat Anti-rabbit IgG (H+L) Alexa Fluor Plus 488	Invitrogen GmbH, Darmstadt, GER
Ki67 monoclonal antibody	Invitrogen GmbH, Darmstadt, GER

2.1.9 Primers

Table 2.9 Primers

Primer name	Sequence 5'-3'
TP53_1F	GGTTCCTGCAATCTGGAACA
TP53_1R	ATTCCCTTCCACCCGGATGA
TP53_2F	TCACCGGGTGGAAAGGGAAT
TP53_2R	GCTGTTACACATGAAGTTGT
TP53_5F	TGCAGCTGTGGGTCAGCTCG
TP53_4R	AACACGCACCTCAAAGCTGT
TP53_5R	CGCCATCCAGTGGCTTCTTC
TP53_9F	TCCTGCAGTACTCCCCTGCC

TP53_6R	GAAGCTAGGAGAGCGTGTC
TP53_8R	TCGGAACATCTCGAAGCGTT
TP53_9R	CAGGTCCTTCTCTCTTGAAC
TP53_11F	AAAATTTCTCAAGAAGGGC
TP53_21F	GTTCAAGAGAGAAGGACCTG
TP53_15F	CTCCATCCTCCCTTTCCTGC
TP53_16F	TCCTGCATGGGGGGCATGAA
TP53_15R	ACTGAGTAAGAGCAGGAAAC
TP53_17F	TGACTGTACCACCATCCACT
TP53_18F	ACAGCTTTGAGGTGCGTGTT
TP53_19F	TTTCCTGCAGTACTCCCCTG
TP53_20F	CCTT TCCTGCAGTA CTCCCCT
TP53_11R	TTGGCCCTTCTTGAGGAAAT
TP53_14F	AGCCCCCTCTGAGTCAGGAG
TP53_10F	ATCCTCCCTTTCCTGCAGTA
TP53_22F	GAAGAAGCCACTGGATGGCG
TP53_23F	A ACGCTTCGAG TGTTCCGA
TP53_24F	ACAACCTCATGTGTAACAGC
TP53_16R	GAGGAAAGGTGAGAAAAGAG
TP53_17R	CAGGAGGTGGCTGGTGTG
TP53_18R	TAGACGGAAATCATAGCTGC
TP53_19R	CGAGCTGACCCACAGCTGCA
TP53_25F	GCAGCTATGATTTCCGTCTA
TP53_27F	ACTGCCACCAGCACCAGCT
TP53_20R	CTATAGTCAGAGCTGCGCTC
TP53_MR5	TCACACAACAACCCCAAATCCTAA
TP53_MF5	TTGTTTTGGTTTGTAGGAAATTTAAT
TP53_MS5	ATAAGAAATTAATAAATTAGG
TP53_MF6	GTTTGGTTTGAAGGAAGGTAGTT
TP53_MR6	ATTCCCTCCACCCAAATAA
TP53_MS6	TGTAGTTGTGGGTTAG
TP53_P21_1F	AGAGGAACTTGGTTAGGTACTTTAGCCACCGCTTTTGGGA
TP53_P21_1R	GCTTTTTGCAAAGCCTAGGATAGGACGCGAAACCTCGTG
TP53_P22_5F	AGAGGAACTTGGTTAGGTACAGTGCAGAGTTGGAGGTCTTA
TP53_P22_2R	GCTTTTTGCAAAGCCTAGGACTGCAGTGGTTTGGGAAGT
TP53_P23_1F	AGAGGAACTTGGTTAGGTACCCTGCCATCAGGAACAACGA
TP53_P23_1R	GCTTTTTGCAAAGCCTAGGAGTGCTCCTCGTGCTTACAC

TP53_P24_1F	AGAGGAACTTGGTTAGGTACGGAGCTTGCCCTTCAGTGAT
TP53_P24_1R	GCTTTTTGCAAAAGCCTAGGCGAGCTGACCCACAGCTGCA
TP53_P11_2F	AGAGGAACTTGGTTAGGTACACCTGTG GCCTATGCAG GTT
TP53_P11_1R	GCTTTTTGCAAAAGCCTAGG GGCCCTGGACTTTTGAGGAG
TP53_MF1	AGTTAAGAATTGGTTGGATGAAAATTTAGA
TP53_MR1	AAACCAATCCCTCAAACCACTAACC
TP53_S1	GGTTGGATGAAAATTTAGATG
TP53_MF2	GTTTTTGTATGGGGGGTATGA
TP53_MR2	AAAAACCTCAACTCCAATAATC
TP53_MS2	GAAGATGTTAGGTAGGG
TP53_pF1	AGGGAGTCCATCTAAAAGTG
TP53_pR1	ACCTCTTCAGAGTAGGTGCT
TP53_pF2	TAGCACAGATGTGGGCAGAA
TP53_pR2	TAGCTCCCAATGATGACAGG
TP53_pF3	AGAGCCTCACCACGGGTGAG
TP53_pR3	CCAGGCACTGTCCCTACGAA
TP53_pF4	TTCGTAGGGACAGTGCCTGG
TP53_pR4	TTCCACCCGGATGAGATGCT
GAPDH_1F	TTCACGACCATGGAGAAGGC
GAPDH_1R	GGTTCACGCCCATCACAAAC
TP73_X4_1F	GGGCCAGGAT TCCCGGAGCT
TP73_X4_1R	CGACGGCGGAAGATCAAAT
TP73_X4_2F	TCCAC CTTCGACACC ATGTC
TP73_X4_2R	TGCTCCGCCCTTCTTGATAGAT
TP73_X4_3F	GGCGGCCCATCCTTATCATC
TP73_X4_3R	CTGCTCGCGGTAGTGATCTT
TP73_X4_4R	CGCCTCTTCTTCACGTTGGT
TP73_X4_4F	GCCAGGTGTGCGAAGATGTC
TP73_X4_5R	TCAGTTGGCCTCGCTCTCTG
TP73_X4_6R	TTTGCTCATGGGTGAGAGGA
TP73_X4_7R	GTTGTTGAGTATCCCTGCGC
TP73_X4_8R	CCCCGAGGTCCTCTATCGTT
TP73_X4_9R	CTCGATGCAGTTTGGACACC
TP73_X4_10R	CAGGCCCTCCTTGATCTTCG
TP73_X4_5F	GGAGAACTTTGAGATCCTCA
TP73_X4_6F	TCCTCTCACCCATGAGCAA
TP73_cmv_4F	CGACTCACTATAGGGGCCGGCCGGCCAGGTGTGCGAAGATG

TP73_cmv_5R	TGTCTGCTCGAAGCGGCCGGCCTCAGTTGGCCTCGCTCTC
TP73_X5_1F	CTTCCACCGCTCCAATGTCA
TP73_X1_1F	ATTCAAACAGAAACTGCCGGG
TP73_X6_1F	TTGTGTCCTGAGAGGGACAGT
TP73_X6_1R	GCCCTACTGCAAAATGGCG
TP73_X8_1F	CCCACATCTTCCAGAGCGTC
TP73_X8_1R	TCCATGGTACTGCTCAGCAA
TP73_X7_1F	TCCTTTACTCTGCTGGGGGA
P73_MF1	GTGGATATAGTAGTAGGGT
P73_MR1	ACCAAAATTACCACTCAAACTCC
P73_MS1	GATATAGTAGTAGGGTTT
P73_prom_1F	CTTGCTCGTACCCCTAAGCC
P73_prom_1R	GTTCGTGCATGATCTCGTCG
TP73_X4_P1.5kb_1F	TGGGTTTGAGTTTTTTGGTGG
TP73_X4_P1.5kb_1R	CACCTCTTTACTACTCACCTACT
P73_x7_pF1	GTTTTGAAGAGTTAAAGGTG
P73_x7_pR1	CCAACAATCCATTCTTTAATAC
P73_x8_pF1	TAGAAGGGTGGTTTTAAAGT
P73_x8_pR1	ACCACCACCCCTTTAA
P73_x7_MS	TTTTTTATGTTTTAGTTAA
P73_x8_MS	AGGGTGGTTTTAAAGTT
TP73_X4_P1.5kb_MS	TTTTTTGGTGGTTTTTT
P73_MS2	TTAGTTTTAGGTAG
P73_prom_2F	CACAGCAGTAGGGCTCCGGC
P73_prom_3F	CCAGTCCCAGGCAGGCGGCC
P73_prom_2R	TGAAGCGAGTGCGGCTGGGC
TP63_X2_1F	GACCCTTACATCCAGCGGTT
TP63_X2_1R	CCTGCATGCGAATACAGTCC
TP63_X2_2R	GGCGTGGTCTGTGTTGTAGG
TP63_X2_2F	CAGTACCTTCCTCAACACACGA
TP63_X2_3R	AGGAAGACTGAGACTGCATCG
TP63_X5_1F	AGGACGTTCTTTGAACTGGCA
TP63_X6_1F	TGGAGCCAGAAGAGAGGACA
TP63_X9_1R	GGCGTCAGATTGTTTCGGGG
gRNA_YAP1_1F	CACCGAGGCAGAAACCATGGATCC
gRNA_YAP1_1R	AAACGGATCCATGGTTTCTGCCTC
YAP1_1F	CAACTAGCTGTCCGGCATCC

YAP1_1R	GGCGAGGTTACCTGTCCG
YAP1_2F	CGTCCGAGGCAAGTTTCTGT
YAP1_2R	GAAAAACAAATCTCGGCCCC
RB1_1F	CCACCGCAGCCTGAGGAGGA
RB1_1R	CCACAGATGAAACCTTCTCC
CDK6_1F	GACCTGAAGAACGGAGGCCG
CDK6_1R	AGTGGTCAAGTCTTGATCAA

2.2 Methods

2.2.1 Molecular biology methods

2.2.1.1 Isolation of plasmid DNA from bacteria (*E. coli*)

Mini prep: bacteria were cultured in 5 ml of medium overnight at 37°C in orbital shaker (220 rpm), centrifuged at max speed (5400xg) for 10 minutes and the supernatant was discarded.

Plasmid isolation without a kit: the bacterial pellet was resuspended in 100 µl miniprep solution I (5 mM sucrose, 10 mM EDTA, 25 mM Tris-HCl pH 8.0). 200 µl of miniprep solution II (0.2 M NaOH, 1 % SDS) was added and mixed by inverting several times. After 3 minutes of incubation at room temperature, 150 µl miniprep solution III (3 M sodium acetate pH 4.8) was added and again mixed by inverting the tube, incubated for 30 minutes on ice, and then centrifuged for 5 minutes. The supernatant was transferred to a 1.5 ml EP tube. After precipitating with 1ml 95% ethanol and a 15-minute centrifugation the pellet was washed first with 500 µl of 80% ethanol followed by 500 µl of 95% ethanol. After each washing step a 10-minute centrifugation at 12000xg was carried out. After removing ethanol, the plasmid DNA pellet was air dried and dissolved in 50 µl water with RNase A (40 µg/ml).

Plasmid isolation with kit: the bacterial pellet was resuspended in 200 µl resuspension buffer and vortexed for 1 minute. 200 µl lysis solution was added and mixed by gentle inversion several times until the mixture was clear and viscous (lysis reaction < 5minutes). And the following steps were according to the protocol from GenElute Plasmid Miniprep Kit (Sigma). Afterwards, the DNA was dissolved in 100 µl elution solution or water.

Midi prep: Midiprep was used to isolate a medium amount of plasmid DNA. 200ml of LB medium was inoculated with bacteria and cultured overnight at 37°C in 220 rpm orbital shaker. Plasmid DNA purification NucleoBond® Xtra Midi Kit was used for the isolation of the

plasmid DNA according to the manufacture's protocol. Afterwards, the DNA was dissolved in 100 µl or 200 µl water.

2.2.1.2 Isolation of mammalian genomic DNA

For tissues: several methods to isolate genomic DNA from tissues were used.

Phenol-chloroform method: first, the tissue was cut into small pieces, moved to a 1.5ml EP tube, 500 µl cell lysis buffer (0,1M Tris, 5mM EDTA, 0,2% SDS, 0,2M NaCl, 100µg/ml Proteinase K) was added and incubated at 37°C overnight. Next day, 500 µl Phenol-chloroform-isoamyl alcohol mixture were added and incubated for 10 minutes at room temperature. After centrifugation for 10 minutes at 12000xg, the supernatant was transferred to a new 1.5 ml EP tube and an equal volume of chloroform was added, mixed, centrifuged for 10 minutes at 12000xg, and the supernatant was transferred to a new 1.5ml EP tube and mixed with 0.7 volume of ice-cold Isopropanol, and centrifuged for 10 minutes at 12000xg. Then the pellet was washed with 200 µl ice cold 70 % ethanol, after the removal of ethanol, the DNA pellet was air dried for 15 minutes. Finally, the pellet was dissolved in 100µl TE buffer.

DNA/RNA AllPrep Mini Kit method: a piece of tissue was cut and placed in a lysis tube (tube P with soft tissue, tube J with hard tissue like bone), 450 µl RTL Plus buffer was added for homogenized 2 times for 30 seconds in Speed Mill PLUS and in between was 10 minutes incubated on ice. Afterwards centrifuged for 5 minutes at 12000xg, and the following steps were according to the protocol from Qiagen Allprep Mini Kit and genomic DNA was eluted with 50 µl TE buffer.

GeneElute Mammalian Genomic DNA kit: tissue was cut in a small piece and then added lysis buffer (with 100µg/ml Proteinase K), incubated at 37°C overnight in the shaker. The following steps were according to the protocol from sigma GeneElute Mammalian Genomic DNA kit and genomic DNA was eluted with 100 µl TE buffer.

For cells: there are mainly two ways to isolated genomic DNA from cells.

Quick Extract: Cell pellets was suspended in 30 µl Quick Extract (QE) buffer (Epicentre) in PCR tubes. The lysis was performed in the PCR machine with 68 °C for 15 min and 95 °C for 8 min. Afterwards 2 µl of the product was used for PCR screening.

DNA/RNA AllPrep Mini Kit method: Cell pellets was suspended in 450 µl RTL Plus buffer and vortexed for 2 minutes, centrifuged for 5 minutes at 12000xg. The following steps were

according to the protocol from Qiagen Allprep Mini Kit and genomic DNA was eluted with 50 μ l TE buffer.

2.2.1.3 Isolation of RNA

For tissues: there are three kits for tissue RNA isolation. Tissues were kept in liquid nitrogen before use and the isolation steps were kept at 4 °C when centrifuged.

InnuSPEED Tissue RNA kit: around 20mg of tissue was cut and placed in a lysis tube (tube P with soft tissue, tube J with hard tissue like bone), 450 μ l lysis buffer was added for homogenized 2 times for 30 seconds in Speed Mill PLUS and in between was 10 minutes incubated on ice. Afterwards centrifuged for 5 minutes at 12000xg, and the following steps were according to the protocol from InnuSPEED Tissue RNA kit. Finally, the RNA was eluted in 40 μ l nuclease-free water.

Trizol RNA isolation: around 20mg of tissue was cut and placed in a lysis tube (tube P with soft tissue, tube J with hard tissue like bone), 450 μ l Trizol was added for homogenized 2 times for 30 seconds in Speed Mill PLUS and in between was 10 minutes incubated on ice. Afterwards centrifuged for 5 minutes at 12000xg, the supernatant was transferred to a new 1.5ml EP tube and equal volume of chloroform was added, mixed, and centrifuged for 5 minutes at 12000xg, and the supernatant was transferred to a new 1.5ml EP tube and the following steps were according to the protocol from InnuSPEED Tissue RNA kit. Finally, the RNA was eluted in 40 μ l nuclease-free water.

DNA/RNA AllPrep Mini Kit method: around 20mg of tissue was cut and placed in a lysis tube (tube P with soft tissue, tube J with hard tissue like bone), 450 μ l RTL Plus buffer was added for homogenized 2 times for 30 seconds in Speed Mill PLUS and in between was 10 minutes incubated on ice. Afterwards centrifuged for 5 minutes at 12000xg, and the following steps were according to the protocol from Qiagen Allprep Mini Kit and RNA was eluted with 40 μ l nuclease-free water.

For cells: Cell pellets was suspended in 450 μ l RTL Plus buffer and vortexed for 2 minutes, centrifuged for 5 minutes at 12000xg. The following steps were according to the protocol from Qiagen Allprep Mini Kit and RNA was eluted with 40 μ l nuclease-free water.

2.2.1.4 DNase treatment

Before reverse transcription, RNA was treated with TURBO DNA-free kit to digest DNA contamination. The steps were according to the protocol from the kit.

2.2.1.5 Quantity and Quality check of nucleic acids

NanoDrop Lite: For standard nucleic acids concentration measurement, 1 µl H₂O was used for blanking, and then 1 µl DNA or RNA was loaded on the Nano drop. The program of dsDNA (factor: 50) and RNA (factor: 40) was applied, and then got the concentration and A260/A280 ratio of each sample, the ratio should be around 1.8 for DNA and 2.0 for RNA.

Qubit 2.0 fluorometer: For more accurate nucleic acids concentration measurement (like for high-throughput sequencing), RNA was measured by the QuantiFluor® RNA System (Promega) (detection range 0.1–500ng) and DNA by Qubit™ dsDNA BR Assay Kit (Thermo Fisher Scientific) (detection range 2- 1000 ng) and Qubit™ dsDNA HS Assay Kit (Thermo Fisher Scientific) (detection range 0.2-100 ng) according to manufacturer's information.

Bioanalyzer kit: For more accurate nucleic acids quality checking, Agilent RNA 6000 Nano kit was used for measuring the RNA integrity number (RIN) according to the kit's protocol. Agilent DNA 1000 Kit and Agilent High Sensitivity DNA Kit was used to detect the Size distribution and quality of sequencing libraries according to the kit's protocol.

2.2.1.6 DNA manipulation

Restriction enzyme digestion

3 to 5 units of enzyme was used for digestion 1 µg of DNA with a final volume of 50 µl. NEB buffer was used for the digestion at the enzyme optimum temperature according to the enzyme's instruction. The standard reaction components for the digestions was shown in table 2.10

Table 2.10 Standard restriction enzyme digestion

Components	Amount
DNA	1-5 µg
10xNEB buffer	5 µl
Enzyme 1	3-5 units/ µg DNA
Enzyme n (if required)	3-5 units/ µg DNA
H ₂ O	up to 50 µl

DNA fragment blunting

DNA fragment sticky ends were blunted by DNA Polymerase I Large Fragment (Klenow) from NEB. The enzyme blunted the fragment by 3' overhangs removal and 5' overhangs fill.

Table 2.11 shows the standard reaction components. Then incubated at 25 °C for 15 minutes and stopped with a final concentration of 10 mM EDTA and heated at 75 °C for 20 minutes.

Table 2.11 Standard Klenow reaction

Components	Amount
DNA	1 to 5 µg
T4 ligase buffer	1x
dNTP	60 µM
Klenow enzyme	2-5 U/µg DNA
T4 ligase	1µl
H ₂ O	up to 25µl

DNA ligation

DNA insert fragment and vector were ligated by T4 DNA ligase. Table 2.12 shows the standard reaction components. Then incubated at room temperature for 1-2 hours or 16°C overnight.

Table 2.12 DNA Ligation

Components	Amount
Insert DNA	$3x(\text{Vector}_{\text{ng}} * \text{size}_{\text{insert}} / \text{size}_{\text{vector}})$
Vector DNA	50-200ng
T4 ligase buffer	1x
T4 ligase	1 µl
H ₂ O	up to 20 µl

Bisulfite Conversion

200 ng of DNA were used for the DNA bisulfite conversion by the EZ DNA Methylation™ Kit's instruction manual. Finally, the converted DNA was eluted in 14 µl M-elution Buffer.

Agarose gel electrophoresis

Agarose gel electrophoresis was performed to separate variable DNA fragments, like PCR product or restriction digested product. 0.8% to 2% gels were made depends on the size of DNA fragments. The gels were melting with a final concentration of 800x peqGreen. TAE gels were run in the 1xTAE buffer, and usually for latter isolation of the DNA fragment. TBE gels were run in the 1xTBE buffer for normal DNA fragment checking. Before loading the

samples into the gel, DNA ladder was loaded to the lanes to show the size of samples. After loading the DNA ladder and samples, the gels ran for 30 minutes to several hours at 80 to 120 voltages depending on the size of the fragments. Visualization of DNA under UV light (366 nm) and photography were carried out by using the *Bio Imaging System Gene Genius*.

Purification of DNA fragments from agarose gels

Targeting DNA fragments were checked from the TAE gel with the visualization of the UV light. Then the DNA fragments were cut from the gel and transferred to 1.5ml EP tubes. Then the DNA was isolated from the gel with the Wizard SV Gel Clean-up System kit according to its instruction manual. The DNA was eluted in 30 µl nuclease free water and stored at -20°C for further research.

Precipitation of DNA with ethanol and sodium chloride

Precipitation of DNA was performed to get sterile DNA for cell culture transfection experiment. 2 volumes of precooled 100% ethanol(-20°C) was added to the DNA solution with 0.1 volume of 3M NaAC and incubated at -20°C overnight. The second day the mixture was centrifuged at 12000xg for 10 minutes and afterwards removed the supernatant. 1 ml 70% sterile ethanol was used to wash the pellet and again centrifuged at 12000xg for 5 minutes, removed the ethanol and air dry the pellet under the laminar flow hood. The pellet was later dissolved in 100 µl low Tris-EDTA solution and measured the concentration and stored at -20°C for further research.

Polymerase Chain Reaction (PCR)

PCR was conducted to get specific DNA fragments from plasmids, cDNA or genomic DNA. Primers were synthesized by Eurofins MWG company and diluted to 10 µM with water for working solution. Different DNA polymerase were used for the amplification with different PCR conditions. Table 2.13 shows the conditions and PCR components with different enzymes.

Table 2.13 PCR components and conditions

Components	Volume (µl)	Temperature (°C)	Time	Cycle
Go Taq PCR				
5x buffer	5	95	3 min	1
dNTPs	0.5	95	30 sec	

Primer F	1	56-65	30 sec	36
Primer R	1	72	1min/kb	
GoTaq	0.25	72	5 min	1
DNA	2	8	forever	
H2O	15.25			

Q5 PCR

10x buffer	5			
10x GC enhancer	5	95	5 min	1
dNTPs	1	95	20 sec	
Primer F	2.5	56-65	20 sec	40
Primer R	2.5	72	30 sec/kb	
GoTaq	0.5	72	5 min	1
DNA	2	8	forever	
H2O	31.5			

Pyromark PCR

2x Master mix	12.5	95	15 min	1
10x buffer	2.5	95	30 sec	
MgCl ₂	0.5	56-65	30 sec	45
Primer F	0.5	72	1min /kb	
Primer R	0.5	72	10 min	1
DNA	2	4	forever	
H2O	6.5			

Phire PCR

5x buffer	10	98	30 sec	1
dNTPs	1	98	5 sec	
Primer F	2	60	5 sec	40
Primer R	2	72	15 sec /kb	
Polymerase	0.5	72	1 min	1
DNA	2	4	forever	
H2O	32.5			

Colony PCR

Colony PCR was used to detect correct recombinant DNA construct. Gotaq PCR mixture was prepared as mentioned above, instead of DNA, the colonies were picked by tooth stick (first transfer to new agar plates for culture) and then mixed with PCR mixture. For detecting fragment longer than 500 bp, first denatured colony with 30 μ l TTE at 95 °C for 5 minutes and took 2 μ l to the PCR mixture.

Mycoplasma Test PCR

Medium were collected from the newly isolated cells of the last three days, heated the medium at 95 °C for 5 minutes and 2 μ l was mixed with the Gotaq PCR mixture with the primers Myco_1F and Myco_1R. 500nM of primer concentration was used and 1.5 mM of MgCl₂ was used in the 25 μ l final volume. PCR program was 2 minutes at 94 °C, 40 cycles of 30 seconds at 94 °C, 30 seconds at 55 °C and 30 seconds at 72 °C, final 3 minutes at 72 °C. Positive control was used from the non-infectious DNA of Mycoplasma genome from the VenorGem Mycoplasma Detection Kit (Sigma-Aldrich Chemie GmbH).

Droplet digital PCR (ddPCR)

Genomic DNA was digested with HindIII (NEB, Frankfurt am Main, Germany) using 3 U/ μ g DNA. TaqMan PCR reaction (23 μ l final volume) was set up using 40 to 100 ng digested DNA, 2 x ddPCR supermix for probes (no dUTP) final concentration 1 x, a 20 x target primer/FAM-labelled probe mix and a 20 x reference primer/HEX labelled probe mix (final concentrations 900 nM each primer, and 250 nM probe). Droplets were generated using a QX200 Droplet Generator combining 20 μ l TaqMan PCR reaction with 70 μ l droplet generator oil for probes in a DG8 Cartridge, then transferred to a PCR Plate (Eppendorf, Hamburg, Germany), the plate sealed and PCR performed in a 96 well thermal cycler with cycling conditions: 95°C for 10 min, followed by 40 cycles of 94°C for 30 s, 61°C for 1 min and a final hold at 98°C for 10 min with 2°C/s ramp rate at all steps. The proportion of PCR- positive to negative droplets was determined using a QX200 droplet reader and data analysed using QuantaSoft Software. Reagents and equipment were from Bio-Rad Laboratories (Hercules, CA, USA), unless otherwise specified.

YAP1 promoter copy number was determined using the fluorescence-labelled *YAP1*-1 probe (5'FAM-cgcgggagggtttaagtgg-BHQ3') and primers *YAP1*-1F (5'-tggtacaggtaccattgtgctcca-3') and *YAP1*-1R (5'-cagtccccgggaaaggttg-3') amplifying a 182 bp fragment. *YAP1* intron 2 copy number was determined using the fluorescence labelled *YAP1*-2 probe (5'FAM-ttctagcgtttgcaaacata-BHQ3') with primers *YAP1*-F2 (5'-agataacataggataggtct-3') and *YAP1*-2R (5'-tgcagagaatgcatagttt-3') amplifying a 147 bp fragment. *YAP1*- 3'UTR copy number was

determined using the fluorescence-labelled YAP1-3 probe (5'FAM-ttgcgaccttctggccaata-BHQ3') and primers YAP1-3F (5'-ccctcaggtagactgcattc-3') and YAP1-3R (5'-gaaagaatcttgctggacgtt-3') amplifying a 138 bp fragment. Porcine *GAPDH*, used as a reference, was detected with the fluorescence-labelled GAPDH probe 5'HEX- tgatgatcaagtctgggtgcc-BHQ3') and primers ddGAPDHF1 (5'-ctcaacgaccacttcgtaa-3') and ddGAPDHR1 (5'-ccctgttgctgtagccaaat-3') amplifying a 181 bp fragment. Primers and probes were from Eurofins Genomic.

Reverse Transcription

200 ng total RNA were converted to cDNA by SuperScript™ II Reverse Transcriptase kit (Invitrogen) according to manufacturer's protocol (Table 2.14). cDNA was diluted to 1:5 with water afterwards.

Table 2.14 RT-PCR components and condition

Components	Volumes
Total RNA	200ng
Random primers	1 µl
dNTPs	1 µl
H ₂ O	up to 12.5 µl
65°C 5 min and then on ice	
0.1M DTT	2 µl
5x Buffer	4 µl
Rnase inhibitor	0.5 µl
25°C 5 min	
Enzyme	1 µl
42°C 50 min; 70°C 15 min	

Quantitative real-time RT-PCR

QPCR was carried out using Kapa SYBR @ Fast Mix (Kapa Biosystems Pty, South Africa) and ABI 7500 PCR System (Applied Biosystems, USA) with default thermal cycling parameters. Reactions were performed in 10 µl volume. Samples were assayed in triplicate; relative expression was normalized to GAPDH expression and fold-differences were calculated by the $\Delta\Delta$ CT method and statistically compared using Students t-test.

Rnase R digestion

RNase R treatment was carried out for 20min at 37°C using 2U RNase R (Epicenter) per 1µg of RNA. Treated RNA was directly reverse transcribed using Superscript IV (Thermo Fisher) with random primers according to the manufacturer's instructions.

5' and 3' Rapid amplification of cDNA ends (RACE)

1 µg total RNA from healthy and OS samples was used for 5' and 3' RACE reactions with the FirstChoice RLM-RACE kit (Ambion) according to manufacturer's protocol. Modified RNA was reverse transcribed using SuperScript IV (Thermo Fisher). The resulting cDNA was used for nested PCR.

Pyrosequencing

Pyrosequencing assays were designed using PyroMark Assay Design 2.0 software (Qiagen). 500 ng genomic DNA was bisulfite-converted with the EZ DNA Methylation-Direct kit (Zymo Research, Irvine, USA) according to the manufacturer's instructions. PCR samples were amplified using PyroMark PCR kit (Qiagen). PCR products were sequenced using PyroMark Q48 Advanced CpG reagents on a PyroMark Q48 Autoprep instrument (Qiagen). For assay optimisation, a methylated (100%), non-methylated (0%) and a scale of control samples with the following DNA methylation: 25%, 50% and 75% were used. The methylated control was prepared using the CpG methyltransferase enzyme (M.SssI; Thermo Scientific). A non-methylated control was prepared using REPLI-g Mini kit (Qiagen).

Next generation RNA sequencing

10 mg of OS and matched healthy samples was used for total RNA extraction using Zymo RNA MiniPrep kit (Zymo Research) according to the manufacturer's instructions. The quality and quantity of RNA samples was measured using an Agilent RNA 6000 Nano kit (Agilent) on a 2100 Bioanalyzer (Agilent) and a Nanodrop 2000 spectrophotometer (Thermo Scientific). The RNA integrity values (RIN) ranged from 7.6 to 9.0. 400 ng total RNA was used for library preparation with the TruSeq RNA Library Preparation Kit v2 (Illumina) according to the manufacturer's instructions, as described in our earlier study [165]. Libraries were sequenced with a HiSeq2500 sequencing system (Illumina) to produce 100-base- paired end reads for 17 samples. An average of 56 million reads per sample were generated. Reads were pseudoaligned against an index of the porcine transcriptome (Sscrofa 11.1; Ensembl release 91) and quantified using *kallisto* (version 0.43.1) [166]. Differential expression of transcripts was quantified using a likelihood-ratio test implemented in the R package *sleuth* (version 0.29.0) [167]. Hierarchical clusters and heat maps for genes with the

most pronounced different levels of expression were generated using the *heatmap.2*-function of the R package *gplots*.

For allele expression imbalance analysis, variant calling based on *STAR* alignments was performed according to GATK best practice recommendations for RNAseq. The GATK tool *Split N Cigar Reads* was used to split reads into exons and remove false variants resulting from overhangs. This step included reassignment of the *STAR* alignment mapping qualities. GATK recalibration of base scores was based on the Ensembl release 83 variant database. Variant calling was carried out using GATK *Haplotype Caller* with the *don't Used Soft Clipped Bases* option. GATK *Variant Filtration* was applied to clusters of at least 3 SNPs within a window of 35 bases between them with the following parameters: Fisher strand value (FS) > 30.0 and a quality by depth value (QD) < 2.0. The probability of allelic imbalance for each SNP was calculated based on the number of reference and alternate allele reads in heterozygous animals using a two-sided binomial test. P values were adjusted for false discovery rate (q value) to take account of multiple testing.

DNA Sequencing

Sequencing was carried out by MWG Eurofins Operon (Ebersberg, Germany). All of samples and primers were prepared according to the company's guidelines.

2.2.2 Microbiological Methods

2.2.2.1 Bacterial culture

Bacteria were cultured on agar plates or in LB medium in incubator or orbital shaker at 220 rpm at 37 °C overnight (< 16 hours). Different antibiotics were added due to the resistance property of the plasmids, like ampicillin (100 µg/ml) or kanamycin (30 µg/ml). The second day the colonies were checked from the culture plate, or the plasmids were isolated from the bacterial liquid.

2.2.2.2 Conservation of bacterial liquid

For conservation of correct colonies, 500 µl 99% glycerol were mixed with 500 µl bacterial liquid and stored at -80 °C for further use.

2.2.2.3 Bacteria transformation

50 µl of DH10b E. coli cells were taken out from -80 °C freezer and thawed on ice. The bacteria cells were mixed with 2 µl ligation products or diluted plasmids, and transferred the

mixture into a cold electroporation cuvette (2 mm gap, Peqlab Biotechnologie GmbH), put into the Multiporator® (Eppendorf) and shocked at 2500 V for 5 msec. The transformed cells were then transferred into a 1.5 ml EP tubes contained 500 ml LB medium and incubated at 37°C in an orbital shaker for around 1 hour at 220rpm. At the same time, agar plates (with ampicillin or kanamycin antibiotics) were put into the incubator at 37°C for drying. After shaking, 200 µl bacterial liquid from the mixture was transferred to the pre-heated agar plates and liquids were evenly distributed with the movement of glass balls. Discarded the glass ball and put the agar plates to the incubator at 37°C. The agar plates were checked by next morning.

2.2.2.4 Blue and white colony screening

Blue and white screening is a rapid and efficient method for identification positive recombinant colonies based on the β-galactosidase by cleaving lactose into glucose and galactose. For recombinant vector, like cloning DNA fragment into the pGEM®-T Easy Vector System (Promega Corporation), 20 µl 100 mg/ml X-gal solution (solved in N, N- dimethylformamid) and 4 µl 1 M IPTG were incubated together with the bacteria cultures on the ampicillin agar plates. And after overnight culture at 37°C, there were two class of colonies: white and blue colonies. White colonies were potential positive colonies which carried pGEM®-T Easy Vector where the lacZ gene was disrupted by incorporated PCR fragment. Blue colonies were negative colonies

2.2.3 Tissue culture methods

All cells were cultivated in a humidified Steri-Cycle incubator in normal condition of 37 °C with 5% CO₂. All the work were handled with sterile equipment and materials in the sterile class II laminar flow hood. Cell culture medium was changed every 2 to 3 days. 0.22 µ filters were used for the sterilization of unsterile solutions. Table 2.15 shows the cell number in each cell culture vessel, the amount of cell medium, accutase.

Table 2.15 Cell culture conditions

Culture vessel	Medium(ml)	Accutase(ml)	Seeding density(10 ⁶)	Confluency number(10 ⁶)
T25 flask	4	1	0.7	2.8
T75 flask	10	3	2.1	8.4
T150 flask	25	5	4.9	23.3
96 well plate	0.1	0.1	0.01	0.04
48 well plate	0.2	0.2	0.03	0.12
24 well plate	0.5	0.3	0.05	0.24

12 well plate	1	0.5	0.1	0.5
6 well plate	2	1	0.3	1.2
10 cm dish	10	5	2.2	8.8
15 cm dish	25	10	5	20

2.2.3.1 Isolation and culture of porcine cells

Before isolation of porcine cells, all the equipment were sterilized and cleaned with 80% ethanol. 0.1mg/ml Penicillin/Streptomycin and 0.1mg/ml Amphotericin B were added to the cell culture medium and PBS.

Isolation and culture of porcine kidney fibroblasts

Cut a piece of kidney (around 0.5 cm³) and removed fat and other tissues, washed 3 times with 80% ethanol, cleaned with PBS and then cut the kidney into small pieces and digested with collagenase Type I-A (Sigma-Aldrich Chemie GmbH) for 30 minutes at 37 °C stirring. Checking whether the tissue was intact or not, if it was still intact, digested for longer time. If it was fine, transferred the digested mixture to a 50ml falcon by 70 µm cell filters. 15 ml pre- cold medium (with Penicillin/Streptomycin and Amphotericin B) was added to stop the collagenase reaction, mixed and then centrifuged at 300 x g for 10 minutes. Discarded the supernatant and resuspended the pellet with another 15 ml medium and then centrifuged again at 300xg for 10 minutes. If the supernatant was still not clean and transparent, repeated the above steps, if it was clean and transparent, then resuspended the cell pellets with culture medium (with Penicillin/Streptomycin and Amphotericin B) and transferred to T75 or T150 flasks depended on the number of cells. Changed the medium on the second and on the fifth day, normal cell culture medium without antibiotics was added to the cells for three days and afterwards the medium was taken for mycoplasma testing.

Isolation and culture of porcine osteosarcoma cells

Pig osteosarcoma cells were isolated from pig tumour bones. 2-3 grams of bone tumour was cut into small pieces and digested with collagenase Type IV (Sigma-Aldrich Chemie GmbH) in gentle MACS Octo Dissociator (Miltenyi Biotec) with program for hard tissue for 2 hours at 37 °C. And the following steps were the same as porcine kidney fibroblasts isolation.

2.2.3.2 Freezing of cells

Cells were washed by PBS for two times and added appropriate accutase (Table 2.6) to detach the cells. When cells were detached, add equal volume of cell culture medium to stop

the reaction and transferred the mixture to a 15 ml falcon. Centrifuged at 300xg for 5 minutes and got the cell pellet by removing the supernatant. The cell pellet was suspended with 1ml freezing buffer (70% FCS, 20% medium and 10% DMSO) and then transferred into a 2 ml cryotube. The cryotubes were immediately transferred to the Mr. Frosty and stored into -80°C freezer, for longer preservation of the cells, the cryotubes were further transferred to the liquid nitrogen.

2.2.3.3 Thawing of cells

The frozen cells were taken out from -80°C freezer or liquid nitrogen and thawed them in a water bath at 37°C. This step had to be fast to reduce the cytotoxicity impact of DMSO, then transferred to a 15 ml falcon containing 3 ml normal cell culture medium, gently mixed and centrifuged at 300xg for 5 minutes and got the cell pellet by removing the supernatant. Suspended the pellet with suitable amount cell culture medium and transferred to new suitable cell culture vessel depends on the cell number and research purposes.

2.2.3.4 Cell Passage

When cells reached 90% confluency, cell passage had to be done. First, removed the medium, cell was washed two times of PBS, added appropriate accutase (Table 2.6) to detach the cells. When cells were fully detached, add equal volume of cell culture medium to stop the reaction. Suspended the cells and took suitable number of cells to a suitable cell culture vessel.

2.2.3.5 Cell counting

When cells were detached and resuspended, added 10 µl suspension cells to a 1.5 ml EP tubes, mixed with 10 µl trypan blue. 10 µl mixture were transferred to the cell counting slide and then put into the cell count machine and afterwards generated the concentration of the total cells and ratio of the live cells.

2.2.3.6 Cell transfection

Electroporation

Cells were washed with PBS for two times and detached and counted, 1×10^6 cells were centrifuged at 300xg for 5 minutes and got the cell pellet by removing the supernatant. Suspended the cell pellet with 100 µl electroporation buffer, added 2 µg plasmid sterile DNA (dissolved in water or low-TE buffer) and transferred to an electroporation cuvette (4mm gap, Peqlab Biotechnologies GmbH). Cells were shocked at 300 Voltages for 100 ms, 1 pulse.

Then the mixture was transferred to a T25 flask with 5 ml normal cell culture medium. After 24 hours, washed with PBS and changed medium.

Nucleofection

Cells were washed with PBS for two times and detached and counted, 0.5×10^6 cells were centrifuged at 300xg for 5 minutes and got the cell pellet by removing the supernatant. Suspended the cell pellet with 100 μ l nucleofection solution, added 2 μ g plasmid sterile DNA (dissolved in water or low-TE buffer) and transferred to a nucleofection cuvette. Cells were shocked by using the program of the Amaxa Nucleofector. Then the mixture was transferred to a T25 flask with 5 ml normal cell culture medium. After 24 hours, washed with PBS and changed medium.

Lipofection

Cells were plating on the 6 well plates one day before the transfection, the second day when the cell confluency reached to 80%, started the lipofectamine 2000 transfection. Cells were washed with PBS for two times and each well changed medium to 0.5 ml opti-men medium. Two 1.5 ml EP tubes were prepared and 150 μ l of opti-men medium was added to each tube. Then added 2 μ l lipofectamine 2000 reagent to one tube, 1 μ g plasmid sterile DNA (dissolved in water or low-TE buffer) to another tube, gently mixed with opti-men medium and incubated for 5 minutes. Then mixed these two tubes, mixed them by pipetting and incubated for another 30 minutes. Afterwards, added this mixture to the 6 well plate drop by drop and put back the 6 well plate to the incubator for 4 to 6 hours and then added 1.5 ml normal cell culture medium to each well. After 24 hours, washed with PBS and changed medium.

2.2.3.7 Cell selection

24 hours after transfection, cells were under antibiotic selection. Different antibiotics and different concentration were used due to the transfection plasmid DNA resistance property and cell types. Most often used antibiotics were Puromycin, Hygromycin and G418. The selection medium changed every 2 to 3 days. The length of the selection depended on the cell type and research purpose. After selection, changed to normal medium or for other use.

2.2.3.8 Cell clone picking

After selection, the cells were transferred to 15 cm dishes, after single cell forming single cell clones of around 100 cells, single cells clones were prepared to pick. First, marked the cell clone with marker at the outside of the dish bottom under microscope. Then washed cells with PBS, discarded PBS and put the sterilized cloning rings on the marked colonies. Added

100 µl accutase to each cloning ring and incubated till the cells fully detached. Transferred these detached cells to 48 well plates and added 200 µl normal cell culture medium to each well.

2.2.3.9 Cell screening

When cells were confluent in wells, detached cells and transferred to 6 well plates. When cells were confluent in 6 well plates, detached cells and one third of the cells were continue cultured in the original well, the rest of the cells were used for genomic DNA or RNA isolation and further screening PCR.

2.2.3.10 Cells for somatic cell nuclear transfer

Selected targeting cell clones were plated on the 96 well plates to reach to 80% of confluency. 48 hours before somatic cell nuclear transfer, washed the cells with PBS 2 times and changed to starvation medium (0.5% FCS medium) to synchronize to G0/G1 phase. The somatic cell nuclear transfer and embryo transfer was conducted by experienced persons.

2.2.3.11 Proliferation assay

5×10^4 transfected cells and control cells ere plated on 6 well plates (3 times for each assay), the cells were detached and counted after 24, 48, 72, 96 and 120 hours of incubation by automated cell counter (Invitrogen)

2.2.3.12 Migration and invasion assay

24 hours before plating, cells were washed and cultured in FCS free medium. 1×10^5 cells were plated on 24-well 8.0 µm transwell inserts (Corning Inc.) directly for cell migration assay, or after coating with 10% Matrigel for the cell invasion assay. Medium with FCS was added at the bottom of each transwell. Cells were incubated for 24 hours, fixed with methanol, stained with Crystal Violet, then washed six times with water, air dried overnight, and the cell number per field was determined. Each experiment was carried out in triplicate.

2.2.3.13 Luciferase reporter assay

Cells were plated into 24-well plates and then transfected with psiCHECK2 plasmids (0.5 µg per well) using Lipofectamine 2000 transfection reagent (Thermo Fischer). An empty psiCHECK2 vector and with the SV40 promoter were used as negative and positive controls. Firefly and Renilla luciferase activities were measured using a Firefly & Renilla Luciferase

Single Tube Assay kit (Biotium) on FLUOstar Omega (BMG Labtech). All assays were performed in triplicate.

2.2.3.14 Immunofluorescence assay

Cells (like porcine OS) were plating in the 6 well plates, cultivate till their confluent, washed cells twice with PBS, fix cells for 15 min at room temperature with Fixative. Wash cells twice with TBST, permeabilize cells for 20 min at room temperature with permeabilization buffer, wash cells twice with TBST, Block unspecific binding sites for 60 min with 5% BAS, apply primary antibody (Ki67 monoclonal antibody, diluted 1:200, MA5-14520, Invitrogen) and incubate at 4°C overnight, wash 3 times with TBST, apply secondary antibody(Goat Anti- rabbit IgG (H+L) Alexa Fluor Plus 488, diluted 1:300; A32731, invitrogen) and incubate for 60 min at room temperature, wash three times with TBST. Add sufficient 300nM DAPI (D9564, sigma), incubate for 10 min at room temperature (protected from the light), remove the staining solution and wash cells 3 times with PBS and cover cells with PBS and detect under Fluorescence Microscope.

2.2.4 Biochemical methods

2.2.4.1 Protein isolation

For tissues: around 20mg of tissue was cut and placed in a lysis tube (tube P with soft tissue, tube J with hard tissue like bone), 200 µl NP40 lysis buffer containing 1x Protease inhibitor (Complete Protease Inhibitor Cocktail, Roche Diagnostic GmbH) was added for homogenized 2 times for 30 seconds and in between was 20 minutes incubated on ice. Afterwards centrifuged at 4 °C for 15 minutes at 12000xg, transferred the supernatant to a new 1.5 ml EP tube and stored at -80 °C freezer.

For cells: around 2 million cells were used for protein isolation. Washed the cells with PBS for 2 times, detached the cells and pelleted the cells. Cells were suspended by 200 µl NP40 lysis buffer containing 1x Protease inhibitor (cComplete Protease Inhibitor Cocktail, Roche Diagnostic GmbH) and transferred the mixture to a 1.5 ml EP tube. Vortexed 2 times for 1 minute and in between was 20 minutes incubated on ice. Afterwards centrifuged at 4 °C for 15 minutes at 12000xg, transferred the supernatant to a new 1.5 ml EP tube and stored at -80 °C freezer.

2.2.4.2 Protein concentration measurement

Protein concentration was measured by Advanced Protein Assay Reagent (Cytoskeleton Inc.). 2 µl protein sample was mixed with 198 µl Advanced Protein Assay Reagent (1:100 dilution) and then transferred to 96 well plates while 2 µl NP40 protein isolation buffer mixed with 198 µl Advanced Protein Assay Reagent (1:100 dilution) was used as a blank. The plate was inserted to the Elisa-Photometer and the concentration was measured with the software at the absorbance of 595 nm. Then calculated the amount of protein for western blots.

2.2.4.3 Western blot analysis

Sodium Dodecyl Sulfate Polyacrylamide Gel

The SDS gel was made with different concentration depending on the size of the targeting protein. All the components were showed in the Table 2.16. First made the separation gel, mixed the buffer and at last added the TEMED, then transferred the mixture to the gel pouring chambers at the position around 70% (the rest 30% is for the collection gel), isopropanol was added to the rest 30% space of the gel chamber to get rid of bubbles. After 20 minutes of full polymerization, removed the isopropanol, prepared the collection gel buffer and also TEMED was the last one to add. And then transferred to the top of separation gel, the Mini-Protean Comb was insert on the top and waited for 20 minutes for the gel to be solid. Then the gel was stored at 4°C in a plastic bag covered with wet tissue or directly used for electrophoresis.

Table 2.16 Components of SDS-polyacrylamide gels

1.5mm gels	Separation gel		Collection gel	
Protein size	<100 kDa	>100 kDa	<100 kDa	>100 kDa
Concentration	12%	10%	6%	4%
Polyacrylamide (40%)	1.8 ml	1.5 ml	250 µl	170 µl
SDS (10%)	60 µl	60 µl	20 µl	20 µl
0.5 M Tris-HCl, pH 6.8			500 µl	500 µl
1 M Tris-HCl, pH 8.8	2.25 ml	2.25 ml		
APS (10%)	60 µl	60 µl	20 µl	20 µl
TEMED	2.4 µl	2.4 µl	2 µl	2 µl
H ₂ O	1.83 ml	2.13 ml	1.21 ml	1.29 ml
Total	6 ml	6 ml	2 ml	2 ml

Protein denaturation and electrophoresis

The biotin protein maker and isolated protein samples were thawed on ice and mixed the protein with 4x Laemmli buffer (DTT added). The mixture was transferred to pcr tubes and denatured at 98°C for 8 minutes in the PCR machine. When the program finished, immediately put the denatured samples on ice, then loaded color marker, biotin marker and other samples to the gel. The electrophoresis ran at 80 V for 30 minutes, then 150 V for 70 minutes.

Western blot

After the electrophoresis, proteins were separated from the gel. The gel was cut at the size of 3.7 cm x 8.5 cm which containing the targeting protein band and transferred the gel to the semi-dry buffer for washing. The PVDF membrane was cut by the same size as the gel, the membrane was activated by methanol for 1 minute and then transferred to the semi-dry buffer. The filter paper was also cut the same size as the gel and transferred to the semi -dry buffer. The blot was assembled on the trans-blot SD semi-dry transfer cell like sandwich. First layer was sponge, put filter paper on the sponge, then the gel on the filter paper, then the PVDF membrane, filter paper and last sponge. Add semi-dry buffer on the sandwich and roller was used to get rid of the buffer in between and closed the trans-blot SD semi-dry transfer cell. Then the blot was running in semi-dry buffer and outside covered with ice, the running time depended on the size of the targeting protein, normally 1 minute for 1 kDa, after that, the proteins were transferred to the PVDF membrane.

Then the membrane was blocked in 1x TBST solution with 5% milk powder or 5% BSA for 1 hour with shaking at room temperature depended on the antibody property, and antibody like mice GAPDH antibody even didn't need blocking. After blocking, washed the membrane with 1x TBST for 3 times, prepared the iBind solution following the manufacturer's instructions from the iBind solution kit (Invitrogen GmbH) and transferred the membrane to the iBind solution with shaking at room temperature. 5 ml of iBind solution was used to wet the iBind card (Invitrogen GmbH) which already lied in the lbind Western System (Invitrogen GmbH). Diluted the first and secondary antibody in iBind solution. Then put the membrane on the membrane part of lbind card (the side with protein towards the card). Closed the lbind Western System and from position 1 to 4 added 2 ml diluted first antibody, 2 ml lbind solution, 2 ml diluted secondary antibody and 5 ml lbind solution. Then incubated for around 4 hours in the lbind Western System.

When incubation finished, the membrane was taken out and transferred to 1x TBST to wash 3 times. Then the membrane was transferred to a plastic foil and covered with 1 ml Pierce

ECL Western Blotting Substrate and then sealed in a western cassette. The cassette and x-ray film were taken to the dark room, in the dark room, suitable size of x-ray film was cut and then put directly on the membrane and closed the western cassette. The film was exposed for several minutes depending on the signal of the protein. Then transferred the film to the developer buffer for 2 minutes, washed with water, and transferred to fix solution for 2 minutes and afterwards washed with water, turned on the light and checked the protein bands on the film. After drying, took the photo.

Immunohistochemistry

Immunohistochemistry was performed as the standard protocol. Samples (like pig OS samples) were fixed in 4% formalin and decalcified in Osteosoft® (Merck). Four-micrometre sections were air-dried for 10 min at 60°C on glass slide. Antigen demasking was performed using the heat retrieval procedure (20 min, citrate buffer pH 6, pressure cooker in microwave medium intensity). Sections were stained with biotinylated antibody (like rabbit anti-YAP1 antibody, diluted 1:200; ARP50530_P050, Aviva System Biology Cooperation) and binding visualized with avidin-peroxidase solution (ABC kit, Vector) followed by DAB staining (Vector). Sections were lightly counterstained with haematoxylin (Merck). Pig duodenum sections were used as a positive control. No incubation with primary antibody was used as a negative control.

2.2.5 Microscopy

Microscopes Axiovert 40CFL and Axiovert 200M (Carl Zeiss Microscopy GmbH) was used to visually assessed the cell morphology, cell viability and confluency as well as fluorescence. Red fluorescent was detected at 554 nm with emission at 581 nm. Green fluorescent was detected at 484 nm with emission at 510 nm. Blue fluorescent was detected at 463 nm with emission at 510 nm. Photographs were taken by the AxioCam HRm and AxioCam MRc cameras and the Axiovision and Axiovision Rel. 4.8 (Carl Zeiss Microscopy GmbH) software.

2.2.6 Necropsy examination and tumour analysis

Pigs were humanely killed and examined by complete necropsy at the Tiergesundheitsdienst Bayern (Bavarian Animal Health Service). In total, 48 OS and matched healthy bone samples from hetero- and homozygous *flTP53^{R167H}* pigs were analysed. For histopathology analysis, organ specimens were fixed in 4% buffered paraformaldehyde, embedded in paraffin, sectioned (3 µm) and stained with haematoxylin and eosin (H&E). Bone specimens were first decalcified in Ossa Fixona (Waldeck GmbH, Germany). For cryosection normal and tumour

samples were frozen in 2-methylbutane (OCT), and for molecular analyses were snap frozen and stored at -80 °C.

2.2.7 Data analysis

2.2.7.1 Statistical Analysis

Graphs generated from qPCR data, CpG methylation data and protein relative expression data were made from Excel with Student T test.

2.2.7.2 Gene set enrichment analysis

Gene set enrichment analysis was conducted by GSEA software (version 2.2.4). The log₂ fold change, adjusted p-Value and the Human Genome Organisation (HUGO) gene symbols were used to generate a preranked file as input for the GSEA Preranked tool. Enrichment analysis was conducted by classic enrichment statistics, 1000 permutations and hallmark gene sets from Molecular Signatures Database (MSigDB) (version 6.1).

3. Results

3.1 Paper I “Porcine model elucidates function of p53 isoform in carcinogenesis and reveals novel *circTP53* RNA”

Guanglin Niu, Isabel Hellmuth, Tatiana Flisikowska, Hubert Pausch, Beate Rieblinger, Alexander Carrapeiro, Benjamin Schade, Brigitte Böhm, Eva Kappe, Konrad Fischer, Bernhard Klinger, Katja Steiger, Reiner Burgkart, Jean-Christophe Bourdon, Dieter Saur, Alexander Kind, Angelika Schnieke, Krzysztof Flisikowski
Oncogene 40 (10), 1896-1908, 2021[168]

Introduction:

This paper revealed that human and porcine *TP53* share similar gene structure, including the internal promoters responsible for expression of *TP53* isoforms. The internal porcine P2 promoter drives expression of the mutant R167H-delta152p53 isoform as well as a newly discovered circular RNA (*circTP53*) in a tissue specific manner. Both were found to play important roles in osteosarcoma development. The other p53 family members-p63 and p73 were also shown to be involved in bone tumorigenesis in pigs. These findings may help to extend the understanding of p53 isoforms and their role in carcinogenesis.

Personal contribution :

Guanglin Niu planned and carried out the experiments shown in Fig 1: RT-PCR, qPCR and WB for the Fig 1b, 1c, 1f and 1g, he did experiments depicted in Fig 2: promoter activity, qPCR, WB, invasion and migration assay for the Fig 2a-2d, 2g, 2i. Promoter activity and methylation results for Fig 3a, 3b. He carried out all experiments shown in Fig 4 for the circRNA study, Fig 5 for the p63 study including qPCR and WB, and Fig 6 for the qPCR and WB of p73 as well as function assay for the p73 and methylation results of p73 promoters.

3.2 Paper II “Allelic expression imbalance analysis identified YAP1 amplification in p53-dependent osteosarcoma”

Guanglin Niu, Agnieszka Bak, Melanie Manyet, Yue Zhang, Hubert Pausch, Tatiana Flisikowska, Angelika E Schnieke, Krzysztof Flisikowski
Cancers 13 (6), 1364, 2021[169]

Introduction:

In this paper, osteosarcoma and healthy bone samples were collected from the same pigs. RNA sequencing and allele expression imbalance analysis was carried out resulting in identification of *YAP1* as a top candidate. Its involvement in p53-dependent osteosarcoma was then confirmed. Experiments were conducted to explore the role of *YAP1* in cell proliferation, migration and invasion. The correlation between *YAP1* and other tumour related genes were also studied on mRNA and protein level. These findings validated the importance of p53/*YAP1* network in tumour development.

Personal contribution :

For the Fig 1, Guanglin Niu planned the experiment, collected samples and prepared the library for the RNA sequencing. He carried out qpcr and WB for the Fig 2d and 2e, and the *YAP1* function assay, Crispr-cas9 knockout of *YAP1*, WB, migration and invasion assay, and immunostaining shown in Fig 3. Guanglin Niu was responsible for all the experiments shown in Fig 4 for the RT-PCR, qpcr and WB and Fig 5 for the methylation results.

3.3 Paper III “Wild-type APC Influences the Severity of Familial Adenomatous Polyposis”

Krzysztof Flisikowski, Carolin Perleberg, **Guanglin Niu**, Thomas Winogrodzki, Agnieszka Bak, Wei Liang, Alessandro Grodziecki, Yue Zhang, Hubert Pausch, Tatiana Flisikowska, Bernhard Klinger, Anna Perkowska, Alexander Kind, Marek Switonski, Klaus-Peter Janssen, Dieter Saur, Angelika Schnieke

Cellular and Molecular Gastroenterology and Hepatology 13 (2), 669-671. e3, 2022[140]

Introduction:

Polyposis severity was found to be variable among *APC*^{1311/+} pigs from the same litter, similar findings have been observed in human patients. In order to explore the genetic reasons for the phenotype, RNA and DNA sequencing was carried out using normal mucosa samples from *APC*^{1311/+} pigs with low or high polyp numbers. A SNP (A/G) from *APC* 3'UTR was found to affect the polyp number, which suggested that wild-type *APC* allele influenced the polyposis. Further experiments were performed to discover the correlation between wild-type *APC* expression level and normal colon epithelium function in *APC*^{1311/+} pigs. Overall, these results give a hint that the *APC* wildtype gene regulates polyposis phenotype and that increased severity level correlates to its altered gene expression.

Personal contribution :

Guanglin Niu contributed to the Fig 1e-1g for the qpcr, WB and DNA methylation results.

4. Discussion

The thesis aimed to analyse the regulation of tumour suppressor genes in two pig cancer models, the *TP53*^{R167H} and *APC*¹³¹¹ models. Section 4.1 discusses the p53 animal model for OS study and section 4.2 the *TP53* promoters and the correlation with methylation level. The role of $\Delta 152p53\alpha$ isoform in cancer is discussed in section 4.3, the role of p53 family members p63 and p73 in tumorigenesis in section 4.4. Section 4.5 discusses the circular *TP53* expression in pigs. Section 4.6 focuses on the differentially expressed genes (DEGs) and allele expression imbalance (AEI) in OS. The functional analysis of *YAP1* is discussed in section 4.7. Section 4.8 discusses the molecular basis of polyposis severity in a porcine model of FAP.

4.1 p53 animal model for osteosarcoma study

p53 is the most studied tumour suppressor gene. *TP53* mutations have been often reported to occur in tumours. However, several aspects of its function are still not clear including the role of its multiple isoforms. In human, it has been well demonstrated that *TP53* expresses at least 9 different mRNA transcripts [170] and at least 12 protein isoforms [171], initiated by three promoters: P1 promoter from the 5' end, Pint1 in intron 1 and P2 in intron 4 as well as alternative splicing through introns 2 and 9; and alternative translation starting site at codons 40, 133 and 160.

In human, the $\Delta 133p53$ and $\Delta 160p53$ isoforms are induced by the internal P2 promoter, but their function in health and disease have not been fully understood. While the function of $\Delta 160p53$ is less studied, the $\Delta 133p53$ is reported to be involved in some cancer types in the regulation of replicative cellular senescence [172], angiogenesis, cytokine secretion/immune response and tumour progression [173]. Together this evidence indicates the important role of the P2 promoter in human p53 related cancers [171].

However, the mouse lacks the P2 promoter which hampers the study of P2 derived p53 isoforms in tumour development, including OS. To overcome this, a mouse model expressing a $\Delta 133p53$ -like protein ($\Delta 122p53$) by the deletion of exon 3 and 4 was developed [174, 175]. Homozygous $\Delta 122p53$ mice show an enhanced proinflammatory phenotype and are prone to develop B-cell tumours [176] with a low incidence of OS (17%) [175]. Although this mouse model does not replicate the situation in human, it strongly supports the notion that p53 isoforms play a role in cancer.

Compared to rodent models, pigs are evolutionary much closer to human [177]. Moreover, the similarities between human and pig in anatomy, physiology, immunology and the metabolic system makes pig a suitable model for studying human diseases, including OS [178]. The study presented here shows that unlike mice, the pig *TP53* has 2 internal promoters, Pint1 in intron 1 and P2 in intron 4 (paper I). The porcine $\Delta 152p53$ isoform originates from P2 promoter which is equivalent to the $\Delta 160p53$ isoform in human. Due to the lack of an additional transcription initiation site in the porcine gene, only the $\Delta 152p53$ isoform was detected in contrast to human where both a $\Delta 133p53$ and $\Delta 160p53$ isoforms exist (paper I). In human, N-terminal splicing has been detected with different isoforms (p53 α,β,χ). In this study, $\Delta 152p53\alpha$ mRNA and N-terminal variants in pigs were detected at different expression in various tumours (paper I).

One other research group has also developed p53 genetically modified pigs which develop OS too. Sieren et al. have generated Yucatan minipigs that carry an R167H mutation in the endogenous *TP53*, which develop a wide spectrum of tumours including osteogenic tumours, lymphomas and renal tumours [129]. In our chair, pigs carrying a latent *TP53*^{R167H} mutation develop a narrow spectrum of tumours, mainly OS [168]. This raised the question why these p53 gene modified pigs have different tumour spectrum and what could be the reason for this narrow spectrum in our pigs. Both pigs can develop OS, but the existence and role of $\Delta 152p53$ in these Yucatan pigs has not been reported. In the Yucatan pigs the selection cassette is inserted in intron 4, which might disturb the activity of the P2 promoter.

4.2 Correlation between DNA methylation and promoter activity in pig *TP53*

The epigenetic study involves a variety of biological processes including tumorigenesis [90]. In this study, the activity of porcine *TP53* promoters, P1, P2 and internal P1 (Pint1) was analysed by luciferase assay and correlated with DNA methylation. A negative correlation between DNA methylation and promoter activity was found in P1, P2 and Pint1 in both osteoblast and osteosarcoma cells in pig *TP53* (paper I). Higher methylation level might block the binding of the transcription factors or complexes which supposed to promote promoter activities. This is an important finding as epigenetic modulation has been reported in regulation of the p53 in both wild type and mutant isoforms in human cancer [179]. However, further investigations need to be conducted to study the role of DNA methylation in gene expression in this scenario.

4.3 Roles of $\Delta 152p53\alpha$ isoform in tumorigenesis

This study shows that porcine $\Delta 152p53\alpha$ mRNA has a similar expression pattern as humans, e.g. higher expression in bone and lack of expression in heart tissue [170]. The finding strongly indicates the narrow tumour spectrum in pigs carrying the floxed $TP53^{R167H}$ allele, mainly OS followed by nephroblastomas and B-cell lymphomas, is related to the higher level of $\Delta 152p53\alpha$ expression in these organs (paper I). This was further confirmed by the discovering that pigs with early onset of OS also had higher expression of the $\Delta 152p53\alpha$ isoform in their healthy bone tissue.

An increase in expression of $\Delta 152p53\alpha$ isoform occurs during tumorigenesis, which is consistent with the p53 isoforms expression in human cancers [11]. The upregulation of human $\Delta 133\Delta/160p53$ variants and their potential oncogenic functions have been reported in lung, colon, breast and ovarian cancers and in melanoma [180-183]. In the pig, wild type and mutant R167H $\Delta 152p53\alpha$ isoforms overexpression can enhance cell proliferation, which is consistent with data for mutant $\Delta 160p53$ isoform in human cancer cells [184]. All this supports the hypothesis that tissue-specific expression of the mutant $\Delta 152p53\alpha$ isoform is driving tumorigenesis in the porcine model and its detection in blood functions as an indicative biomarker.

4.4 Expression of p53 family members in porcine osteosarcoma

Increasing evidence suggests that mutant p53 gain of function is based on its interaction with p63 and p73 [185, 186], as well as the ratio of TA/ ΔN p63/p73 isoforms which determines their effect on tumorigenesis [187, 188].

p63 has a very low mutation rate compared to p53, but was also reported to play a role in tumorigenesis. It has two major isoforms, TAp63 and $\Delta Np63$ [30]. While TAp63 is considered to be a tumour suppressor, $\Delta Np63$ is an oncogene [31-33]. In this study, there is no expression change between healthy bone and tumour tissue on both mRNA and protein level, which indicates that there is no effect of $\Delta Np63$ on OS development. However, in kidney and spleen samples TAp63 δ was expressed significantly higher in those tumours compared to normal tissue, which indicates its potential functions in kidney and spleen tumours as well as its tissue-specific property.

p73 also has two major isoforms, TAp73 and Δ Np73. To have a better understanding of p73, both TAp73 specific and Δ Np73 specific knockout mice were generated. TAp73 knockout mice show partial embryonic lethality, infertility and increased spontaneous and induced carcinogenesis, this may partly be due to the absence of TAp73 [189]. In contrast, Δ Np73 deficiency mice exhibit no evidence of tumour development, and Δ Np73 deficiency mouse fibroblast cells fail to form tumours after transplanting into immunocompromised mice [190]. These observations afford TAp73, like p53, a role of tumour suppresser, and an oncogenic function for Δ Np73.

p73 is involved in many tumours, like breast, ovarian, colon cancers and so on [40-42]. In breast cancer, both TAp73 and Δ Np73 are upregulated, but in ovarian cancer, only TAp73 isoform is upregulated while in colon cancer only Δ Np73 is upregulated. The function of TAp73 and Δ Np73 differs among tumours.

As mentioned in the introduction, TAp73 is the major isoform in human OS cell—SAOS2, which is consistent with our results that TAp73 is the predominant isoform in pig OS (paper I). We detected a higher expression of TAp73 in pig OS compare to normal bones, this also coincides with the study previously mentioned which shows that in human 1/3 of OS specimens have a higher expression of TAp73 compared to normal tissues [52]. Based on the results of western blots, TAp73 has higher expression in bone tumours which might indicate the possible function of TAp73 in tumorigenesis in pigs, especially for bone tissue.

Overall, upregulation of the TAp63 δ and TAp73 δ isoforms was detected in all studied tumours, and *in vitro* expression of the TAp73 δ isoform promoted the proliferation of human and porcine OS cells. However, further work is required to prove the direct interaction and regulation among these isoforms.

4.5 Circular *TP53* expression in pigs

Circular RNAs, one class of non-coding RNAs, play an important role in biological processes including tumorigenesis [191]. The tumorigenic function of some circular RNAs in OS has also been reported. Upregulation of circRNAs such as *circNASP*, *circPVT1*, Hsa_circ_0016347, *circNT5C2*, Hsa_circ_0001564, Hsa_circ_0009910, *circUBAP2*, *circGLI2* and Hsa_circ_0008717 was observed in human OS. The circRNAs regulate the cell proliferation, cell cycle, tumour invasion and metastasis, and also serve as diagnostic and therapeutic biomarkers and as potential therapeutic target for reducing OS growth [191].

Circular RNAs like *circHIPK2* and Hsa_circ_0002052 were downregulated in OS, suggesting their tumour-suppressive function in OS [191].

In this study the *circTP53* expressed from the P2 promoter was identified. It has not previously been described for human and would be absent in mice, which lack the P2 promoter. It is upregulated in OS together with its parental $\Delta 152p53\alpha$ isoform. *In vitro* studies showed that high *circTP53* expression increases cellular proliferation of OS cells (paper I). Similar mechanisms of circRNAs were described for other genes as referenced above (paper I). However, the mechanism of how *circTP53* affects cell proliferation is still unknown and needs further investigation. In the future, the deep next-generation sequencing should be applied to obtain a compelling view on circular *TP53* expression in OS and other tumours.

4.6 Next-generation sequencing and AEI analysis reveals *YAP1* function in osteosarcoma

To further analyse the genetic factors contributing to OS development in the *TP53^{R167H}* pigs, RNA sequencing and allele expression imbalance (AEI) analysis have been carried out using OS and matched healthy tissue. The RNA sequencing technique has been applied to detect driver mutations in human OS in several studies [74, 80, 192]. Several well-known cancer driver genes such as *TP53*, *RB1*, *BRCA1*, *PTEN*, *ATRX* as well as passenger mutations have been identified [73]. The AEI quantifies the differences in the expression of two alleles of a genetic locus [193-195] or two haplotypes of a diploid individual that can be distinguished at heterozygous variant loci [196]. Compared to standard gene expression analysis, AEI has the advantage of using two alleles of a gene within an individual, thus better controlling for genetic background and environmental influences, and therefore allowing sensitive and accurate detection of genetic and epigenetic differences in highly heterocellular samples such as tumours [197, 198]. In this work, AEI analysis was applied to reduce the impact of the tumour heterogeneity on the gene expression. It indicated that *YAP1* amplification may play an important role in OS progression in p53-deficient pigs. The *YAP1* amplification leads to an upregulation of *YAP1* in the cell nucleus and correlates with OS progression (paper II). This is consistent with previous studies showing an increased expression of *YAP1*, which is associated with poor prognosis and chemical resistance in human OS [57, 87]. Noteworthy, downregulation of *YAP1* has been reported to reduce the oncogenic potential of human OS cells [86, 199].

4.7 *YAP1* in osteosarcoma development

Here, *YAP1* expression was associated with gene amplification in p53 deficient porcine OS. The amplification of *YAP1* has been reported in different cancers including medulloblastoma [200], brain cancer [201] and oesophageal squamous cell carcinoma [202]. The interplay between p53 and *YAP1* has also been detected in pancreatic cancer (PDAC) where p53-deficiency promoted *YAP1* activity [203, 204], and *YAP1* deletion blocked PDAC initiation driven by *KRAS* and *p53* mutations [205]. In this study, *YAP1* deficiency was found to reduce the tumorigenic potential of p53 deficient OS cells.

The regulatory role for the p53 and *YAP1* pathway in mediating the tumorigenesis has been reported [58]. *YAP1* has been shown to interact with mutant p53, including the R175H mutation [206]. Also, nuclear localisation and activity of *YAP1* is dependent on p53. While tumours with wild-type *TP53* lack *YAP1* nuclear localisation in pancreatic cancer [203], loss of p53 in mutant *KRAS*^{G12D} lung cancer leads to increased nuclear localisation of *YAP1* [207]. A high activity of nuclear *YAP1* was showed in OS from *fITP53*^{R167H} pigs (paper II). Importantly, the nuclear *YAP1* localisation was negatively associated with survival in OS patients [57]. Together, these findings suggest an interaction between mutant p53 isoform and *YAP1* in pig OS. Further validation of this interaction needs to be applied.

For p53 family members, *YAP1* was reported to physically interact with p63, p73 [58], and regulate the p53/Rb1/p16 dependent cellular pathways [208]. The Δ Np63 isoform regulates *YAP1* translocation in squamous carcinoma [209], and in response to DNA damage. *YAP1* functions as a transcriptional cofactor of p73-mediated apoptosis [210]. Consistent with these data, the knockout of *YAP1* in p53-deficient OS cells was found to downregulates p63 and upregulates *p16* and *RB1* (paper II). In addition, this study showed that *YAP1* deletion reduced the *p16* promoter methylation, similar findings were observed in *YAP1*-deficient mouse pancreatic tumour cells [204].

In summary, this study demonstrates the role of *YAP1* in the progression of p53-dependent OS, which in turn provides an additional step to better understand the function of the p53/*YAP1* network in cancer.

4.8 Wild-type *APC* in Familial Adenomatous Polyposis

Germline mutation in the *APC* gene is the cause for FAP. The *APC*^{1311/+} pig model generated by our chair recapitulates the main features of the human disease [135]. Like in human patients, the polyposis varies between *APC*^{1311/+} siblings. This study focused on the genetic basis for the phenotype difference.

RNA sequencing was applied to identify differentially expressed genes in normal mucosa samples from *APC*^{1311/+} pigs with low or high polyp number. However, the only significant gene detected, named cholesterol 7 alpha-hydroxylase (*CYP7A1*), had been correlated with colon inflammation, and no difference in non-inflamed colon mucosa of young *APC*^{1311/+} pigs was observed (paper III). Wild-type *APC* expression has been reported to drives the CRC cells into apoptosis. Here we aimed to study if *APC* itself could affect the polyposis variance. DNA sequencing was conducted, and SNPs were detected in the 3' UTR only. One SNP (C.10046A/G) was in the conserved recognition site for miR17-5P (paper III), which had previously been reported to play a role in colorectal cancer in humans. The mutant allele showed adenine(A*) while wild type was either guanine(G) or adenine(A). More polyps were found in A*G genotypes compared to A*A (paper III). The mutant *APC*¹³¹¹ allele generates a shortened mRNA and a truncated protein. In normal mucosa, the G allele expression was reduced by 2 folds on both mRNA and protein level. The reason was the SNP in the 3' UTR, which was further confirmed via a luciferase assay. This sequence also showed a higher methylation level in the A*G genotype (Paper III).

Further functional assays showed increased mucosa thickness in A*G genotypes, higher level of Ki67 positive cells, higher expression of LGR5 (colon stem cell marker) as well as increased organoids formation abilities (Paper III).

In conclusion, in the *APC*¹³¹¹ model, expression of truncated *APC* combined with reduced expression of wild-type allele resulted in polyposis, which is consistent with the previous report that reduced expression of *APC* mRNA is related to the polyp formation in human FAP patients. This proves the importance of *APC* expression levels in the regulation of FAP.

In summary: mouse models have helped to understand the molecular basis of many diseases, but like all models they fail to replicate all aspects of human genetics or physiology. With my thesis I could show that pig models might be able to fill the gap and enables us to study mechanism of tumorigenesis which differ between human and mouse. In recent years, more and more porcine models of different cancers and diseases have been generated, not only for basic medical research, but also for the translational medicine. In the long-term battle against human cancer, both physicians and researchers will gain a better understanding of the pathogenesis of the diseases through porcine models and species comparison.

5. Reference

1. Levine, A.J., *p53: 800 million years of evolution and 40 years of discovery*. Nat Rev Cancer, 2020. **20**(8): p. 471-480.
2. Belyi, V.A., et al., *The origins and evolution of the p53 family of genes*. Cold Spring Harb Perspect Biol, 2010. **2**(6): p. a001198.
3. Ho, T., B.X. Tan, and D. Lane, *How the Other Half Lives: What p53 Does When It Is Not Being a Transcription Factor*. Int J Mol Sci, 2019. **21**(1).
4. Yoh, K. and R. Prywes, *Pathway Regulation of p63, a Director of Epithelial Cell Fate*. Front Endocrinol (Lausanne), 2015. **6**: p. 51.
5. Deutsch, G.B., et al., *DNA damage in oocytes induces a switch of the quality control factor TAp63alpha from dimer to tetramer*. Cell, 2011. **144**(4): p. 566-76.
6. Vousden, K.H. and D.P. Lane, *p53 in health and disease*. Nat Rev Mol Cell Biol, 2007. **8**(4): p. 275-83.
7. Wang, X., E.R. Simpson, and K.A. Brown, *p53: Protection against Tumor Growth beyond Effects on Cell Cycle and Apoptosis*. Cancer Res, 2015. **75**(23): p. 5001-7.
8. Wawryk-Gawda, E., et al., *P53 protein in proliferation, repair and apoptosis of cells*. Protoplasma, 2014. **251**(3): p. 525-33.
9. Aubrey, B.J., et al., *How does p53 induce apoptosis and how does this relate to p53-mediated tumour suppression?* Cell Death Differ, 2018. **25**(1): p. 104-113.
10. Chen, J., *The Cell-Cycle Arrest and Apoptotic Functions of p53 in Tumor Initiation and Progression*. Cold Spring Harb Perspect Med, 2016. **6**(3): p. a026104.
11. Anbarasan, T. and J.C. Bourdon, *The Emerging Landscape of p53 Isoforms in Physiology, Cancer and Degenerative Diseases*. Int J Mol Sci, 2019. **20**(24).
12. Purdie, C.A., et al., *Tumour incidence, spectrum and ploidy in mice with a large deletion in the p53 gene*. Oncogene, 1994. **9**(2): p. 603-9.
13. Jacks, T., et al., *Tumor spectrum analysis in p53-mutant mice*. Curr Biol, 1994. **4**(1): p. 1-7.
14. Donehower, L.A., et al., *Mice deficient for p53 are developmentally normal but susceptible to spontaneous tumours*. Nature, 1992. **356**(6366): p. 215-21.
15. Lavigne, A., et al., *High incidence of lung, bone, and lymphoid tumors in transgenic mice overexpressing mutant alleles of the p53 oncogene*. Mol Cell Biol, 1989. **9**(9): p. 3982-91.
16. Lee, J.M., et al., *Susceptibility to radiation-carcinogenesis and accumulation of chromosomal breakage in p53 deficient mice*. Oncogene, 1994. **9**(12): p. 3731-6.
17. Harvey, M., et al., *A mutant p53 transgene accelerates tumour development in heterozygous but not nullizygous p53-deficient mice*. Nat Genet, 1995. **9**(3): p. 305-11.
18. Brosh, R. and V. Rotter, *When mutants gain new powers: news from the mutant p53 field*. Nat Rev Cancer, 2009. **9**(10): p. 701-13.
19. Muller, P.A. and K.H. Vousden, *p53 mutations in cancer*. Nat Cell Biol, 2013. **15**(1): p. 2-8.
20. Olive, K.P., et al., *Mutant p53 gain of function in two mouse models of Li-Fraumeni syndrome*. Cell, 2004. **119**(6): p. 847-60.
21. Tong, C., et al., *Production of p53 gene knockout rats by homologous recombination in embryonic stem cells*. Nature, 2010. **467**(7312): p. 211-3.
22. Huang, G., et al., *Beyond knockout rats: new insights into finer genome manipulation in rats*. Cell Cycle, 2011. **10**(7): p. 1059-66.
23. van Boxtel, R., et al., *Homozygous and heterozygous p53 knockout rats develop metastasizing sarcomas with high frequency*. Am J Pathol, 2011. **179**(4): p. 1616-22.
24. Cheng, R., et al., *Zebrafish (Danio rerio) p53 tumor suppressor gene: cDNA sequence and expression during embryogenesis*. Mol Mar Biol Biotechnol, 1997. **6**(2): p. 88-97.
25. Ignatius, M.S., et al., *tp53 deficiency causes a wide tumor spectrum and increases embryonal rhabdomyosarcoma metastasis in zebrafish*. Elife, 2018. **7**.

26. Berghmans, S., et al., *tp53 mutant zebrafish develop malignant peripheral nerve sheath tumors*. Proc Natl Acad Sci U S A, 2005. **102**(2): p. 407-12.
27. Mizgireuv, I.V. and S.Y. Revskoy, *Transplantable tumor lines generated in clonal zebrafish*. Cancer Res, 2006. **66**(6): p. 3120-5.
28. Levine, A.J., *p53: 800 million years of evolution and 40 years of discovery*. Nat Rev Cancer, 2020.
29. Bergholz, J. and Z.X. Xiao, *Role of p63 in Development, Tumorigenesis and Cancer Progression*. Cancer Microenviron, 2012. **5**(3): p. 311-22.
30. Melino, G., *p63 is a suppressor of tumorigenesis and metastasis interacting with mutant p53*. Cell Death Differ, 2011. **18**(9): p. 1487-99.
31. Flores, E.R., et al., *Tumor predisposition in mice mutant for p63 and p73: evidence for broader tumor suppressor functions for the p53 family*. Cancer Cell, 2005. **7**(4): p. 363-73.
32. Keyes, W.M., et al., *p63 heterozygous mutant mice are not prone to spontaneous or chemically induced tumors*. Proc Natl Acad Sci U S A, 2006. **103**(22): p. 8435-40.
33. Su, X., et al., *TAp63 suppresses metastasis through coordinate regulation of Dicer and miRNAs*. Nature, 2010. **467**(7318): p. 986-90.
34. Yi, M., et al., *TP63 links chromatin remodeling and enhancer reprogramming to epidermal differentiation and squamous cell carcinoma development*. Cell Mol Life Sci, 2020. **77**(21): p. 4325-4346.
35. Vousden, K.H. and C. Prives, *Blinded by the Light: The Growing Complexity of p53*. Cell, 2009. **137**(3): p. 413-31.
36. Melino, G., V. De Laurenzi, and K.H. Vousden, *p73: Friend or foe in tumorigenesis*. Nat Rev Cancer, 2002. **2**(8): p. 605-15.
37. Irwin, M.S., *DeltaNp73: misunderstood protein?* Cancer Biol Ther, 2006. **5**(7): p. 804-7.
38. Conforti, F., et al., *Relative expression of TAp73 and DeltaNp73 isoforms*. Aging (Albany NY), 2012. **4**(3): p. 202-5.
39. Moll, U.M., *The Role of p63 and p73 in tumor formation and progression: coming of age toward clinical usefulness. Commentary re: F. Koga et al., Impaired p63 expression associates with poor prognosis and uroplakin III expression in invasive urothelial carcinoma of the bladder. Clin. Cancer Res., 9: 5501-5507, 2003, and P. Puig et al., p73 Expression in human normal and tumor tissues: loss of p73alpha expression is associated with tumor progression in bladder Cancer. Clin. Cancer Res., 9: 5642-5651, 2003. Clin Cancer Res, 2003. 9(15): p. 5437-41.*
40. Rufini, A., et al., *p73 in Cancer*. Genes Cancer, 2011. **2**(4): p. 491-502.
41. Uboveja, A., et al., *p73 - NAV3 axis plays a critical role in suppression of colon cancer metastasis*. Oncogenesis, 2020. **9**(2): p. 12.
42. Mitkin, N.A., et al., *p63 and p73 repress CXCR5 chemokine receptor gene expression in p53-deficient MCF-7 breast cancer cells during genotoxic stress*. Biochim Biophys Acta Gene Regul Mech, 2017. **1860**(12): p. 1169-1178.
43. Amelio, I., et al., *TAp73 opposes tumor angiogenesis by promoting hypoxia-inducible factor 1alpha degradation*. Proc Natl Acad Sci U S A, 2015. **112**(1): p. 226-31.
44. Stantic, M., et al., *TAp73 suppresses tumor angiogenesis through repression of proangiogenic cytokines and HIF-1alpha activity*. Proc Natl Acad Sci U S A, 2015. **112**(1): p. 220-5.
45. Dulloo, I., et al., *Hypoxia-inducible TAp73 supports tumorigenesis by regulating the angiogenic transcriptome*. Nat Cell Biol, 2015. **17**(4): p. 511-23.
46. Dulloo, I., P.B. Hooi, and K. Sabapathy, *Hypoxia-induced DNp73 stabilization regulates Vegf-A expression and tumor angiogenesis similar to TAp73*. Cell Cycle, 2015. **14**(22): p. 3533-9.
47. Fernandez-Alonso, R., et al., *p73 is required for endothelial cell differentiation, migration and the formation of vascular networks regulating VEGF and TGFbeta signaling*. Cell Death Differ, 2015. **22**(8): p. 1287-99.
48. Du, W., et al., *TAp73 enhances the pentose phosphate pathway and supports cell proliferation*. Nat Cell Biol, 2013. **15**(8): p. 991-1000.

49. Chen, X., et al., *p73 is transcriptionally regulated by DNA damage, p53, and p73*. *Oncogene*, 2001. **20**(6): p. 769-74.
50. Fogh, J., J.M. Fogh, and T. Orfeo, *One hundred and twenty-seven cultured human tumor cell lines producing tumors in nude mice*. *J Natl Cancer Inst*, 1977. **59**(1): p. 221-6.
51. Kommagani, R., et al., *p73 is essential for vitamin D-mediated osteoblastic differentiation*. *Cell Death Differ*, 2010. **17**(3): p. 398-407.
52. Park, H.R., et al., *Low expression of p63 and p73 in osteosarcoma*. *Tumori*, 2004. **90**(2): p. 239-43.
53. Vikhрева, P., G. Melino, and I. Amelio, *p73 Alternative Splicing: Exploring a Biological Role for the C-Terminal Isoforms*. *J Mol Biol*, 2018. **430**(13): p. 1829-1838.
54. Harvey, K.F., C.M. Pflieger, and I.K. Hariharan, *The Drosophila Mst ortholog, hippo, restricts growth and cell proliferation and promotes apoptosis*. *Cell*, 2003. **114**(4): p. 457-67.
55. Sudol, M., *Yes-associated protein (YAP65) is a proline-rich phosphoprotein that binds to the SH3 domain of the Yes proto-oncogene product*. *Oncogene*, 1994. **9**(8): p. 2145-52.
56. Chen, X., et al., *Molecular Mechanism of Hippo-YAP1/TAZ Pathway in Heart Development, Disease, and Regeneration*. *Front Physiol*, 2020. **11**: p. 389.
57. Bouvier, C., et al., *Prognostic value of the Hippo pathway transcriptional coactivators YAP/TAZ and beta1-integrin in conventional osteosarcoma*. *Oncotarget*, 2016. **7**(40): p. 64702-64710.
58. Raj, N. and R. Bam, *Reciprocal Crosstalk Between YAP1/Hippo Pathway and the p53 Family Proteins: Mechanisms and Outcomes in Cancer*. *Front Cell Dev Biol*, 2019. **7**: p. 159.
59. Su, X., et al., *TAp63 suppresses mammary tumorigenesis through regulation of the Hippo pathway*. *Oncogene*, 2017. **36**(17): p. 2377-2393.
60. Strano, S., et al., *Physical interaction with Yes-associated protein enhances p73 transcriptional activity*. *J Biol Chem*, 2001. **276**(18): p. 15164-73.
61. Groden, J., et al., *Identification and characterization of the familial adenomatous polyposis coli gene*. *Cell*, 1991. **66**(3): p. 589-600.
62. Nathke, I.S., *The adenomatous polyposis coli protein: the Achilles heel of the gut epithelium*. *Annu Rev Cell Dev Biol*, 2004. **20**: p. 337-66.
63. Aghabozorgi, A.S., et al., *Role of adenomatous polyposis coli (APC) gene mutations in the pathogenesis of colorectal cancer; current status and perspectives*. *Biochimie*, 2019. **157**: p. 64-71.
64. Schaefer, K.N. and M. Peifer, *Wnt/Beta-Catenin Signaling Regulation and a Role for Biomolecular Condensates*. *Dev Cell*, 2019. **48**(4): p. 429-444.
65. Dogterom, M. and G.H. Koenderink, *Actin-microtubule crosstalk in cell biology*. *Nat Rev Mol Cell Biol*, 2019. **20**(1): p. 38-54.
66. Spier, I., et al., *Low-level APC mutational mosaicism is the underlying cause in a substantial fraction of unexplained colorectal adenomatous polyposis cases*. *J Med Genet*, 2016. **53**(3): p. 172-9.
67. Aitchison, A., et al., *APC Mutations Are Not Confined to Hotspot Regions in Early-Onset Colorectal Cancer*. *Cancers (Basel)*, 2020. **12**(12).
68. Luetke, A., et al., *Osteosarcoma treatment - where do we stand? A state of the art review*. *Cancer Treat Rev*, 2014. **40**(4): p. 523-32.
69. Ottaviani, G. and N. Jaffe, *The epidemiology of osteosarcoma*. *Cancer Treat Res*, 2009. **152**: p. 3-13.
70. Hung, G.Y., et al., *Improvement in High-Grade Osteosarcoma Survival: Results from 202 Patients Treated at a Single Institution in Taiwan*. *Medicine (Baltimore)*, 2016. **95**(15): p. e3420.
71. Custodio, G., et al., *Impact of neonatal screening and surveillance for the TP53 R337H mutation on early detection of childhood adrenocortical tumors*. *J Clin Oncol*, 2013. **31**(20): p. 2619-26.

72. Varley, J.M., *Germline TP53 mutations and Li-Fraumeni syndrome*. Hum Mutat, 2003. **21**(3): p. 313-20.
73. Rickel, K., F. Fang, and J. Tao, *Molecular genetics of osteosarcoma*. Bone, 2017. **102**: p. 69-79.
74. Chen, X., et al., *Recurrent somatic structural variations contribute to tumorigenesis in pediatric osteosarcoma*. Cell Rep, 2014. **7**(1): p. 104-12.
75. Rausch, T., et al., *Genome sequencing of pediatric medulloblastoma links catastrophic DNA rearrangements with TP53 mutations*. Cell, 2012. **148**(1-2): p. 59-71.
76. Maciejowski, J., et al., *Chromothripsis and Kataegis Induced by Telomere Crisis*. Cell, 2015. **163**(7): p. 1641-54.
77. Morishita, M., et al., *Chromothripsis-like chromosomal rearrangements induced by ionizing radiation using proton microbeam irradiation system*. Oncotarget, 2016. **7**(9): p. 10182-92.
78. Futreal, P.A., et al., *A census of human cancer genes*. Nat Rev Cancer, 2004. **4**(3): p. 177-83.
79. Martinez-Jimenez, F., et al., *A compendium of mutational cancer driver genes*. Nat Rev Cancer, 2020. **20**(10): p. 555-572.
80. Kovac, M., et al., *Exome sequencing of osteosarcoma reveals mutation signatures reminiscent of BRCA deficiency*. Nat Commun, 2015. **6**: p. 8940.
81. Perry, J.A., et al., *Complementary genomic approaches highlight the PI3K/mTOR pathway as a common vulnerability in osteosarcoma*. Proc Natl Acad Sci U S A, 2014. **111**(51): p. E5564-73.
82. Berman, S.D., et al., *Metastatic osteosarcoma induced by inactivation of Rb and p53 in the osteoblast lineage*. Proc Natl Acad Sci U S A, 2008. **105**(33): p. 11851-6.
83. Ballatori, S.E. and P.W. Hinds, *Osteosarcoma: prognosis plateau warrants retinoblastoma pathway targeted therapy*. Signal Transduct Target Ther, 2016. **1**: p. 16001.
84. Nielsen, G.P., et al., *CDKN2A gene deletions and loss of p16 expression occur in osteosarcomas that lack RB alterations*. Am J Pathol, 1998. **153**(1): p. 159-63.
85. Moriarity, B.S., et al., *A Sleeping Beauty forward genetic screen identifies new genes and pathways driving osteosarcoma development and metastasis*. Nat Genet, 2015. **47**(6): p. 615-24.
86. Chan, L.H., et al., *Hedgehog signaling induces osteosarcoma development through Yap1 and H19 overexpression*. Oncogene, 2014. **33**(40): p. 4857-66.
87. Wang, D.Y., et al., *Hippo/YAP signaling pathway is involved in osteosarcoma chemoresistance*. Chin J Cancer, 2016. **35**: p. 47.
88. Yang, Z., et al., *Knockdown of YAP1 inhibits the proliferation of osteosarcoma cells in vitro and in vivo*. Oncol Rep, 2014. **32**(3): p. 1265-72.
89. de Azevedo, J.W.V., et al., *Biology and pathogenesis of human osteosarcoma*. Oncol Lett, 2020. **19**(2): p. 1099-1116.
90. Sachdeva, M., et al., *Epigenetic silencing of Kruppel like factor-3 increases expression of pro-metastatic miR-182*. Cancer Lett, 2015. **369**(1): p. 202-11.
91. Sharma, S., T.K. Kelly, and P.A. Jones, *Epigenetics in cancer*. Carcinogenesis, 2010. **31**(1): p. 27-36.
92. Kanherkar, R.R., N. Bhatia-Dey, and A.B. Csoka, *Epigenetics across the human lifespan*. Front Cell Dev Biol, 2014. **2**: p. 49.
93. Tang, N., et al., *Osteosarcoma development and stem cell differentiation*. Clin Orthop Relat Res, 2008. **466**(9): p. 2114-30.
94. Varshney, J., et al., *Understanding the Osteosarcoma Pathobiology: A Comparative Oncology Approach*. Vet Sci, 2016. **3**(1).
95. Jeziorska, D.M., et al., *DNA methylation of intragenic CpG islands depends on their transcriptional activity during differentiation and disease*. Proc Natl Acad Sci U S A, 2017. **114**(36): p. E7526-E7535.
96. Li, B. and Z. Ye, *Epigenetic alterations in osteosarcoma: promising targets*. Mol Biol Rep, 2014. **41**(5): p. 3303-15.

97. Rao-Bindal, K. and E.S. Kleinerman, *Epigenetic regulation of apoptosis and cell cycle in osteosarcoma*. *Sarcoma*, 2011. **2011**: p. 679457.
98. Bannister, A.J. and T. Kouzarides, *Regulation of chromatin by histone modifications*. *Cell Res*, 2011. **21**(3): p. 381-95.
99. Li, S., *Implication of posttranslational histone modifications in nucleotide excision repair*. *Int J Mol Sci*, 2012. **13**(10): p. 12461-86.
100. Kelly, T.K., D.D. De Carvalho, and P.A. Jones, *Epigenetic modifications as therapeutic targets*. *Nat Biotechnol*, 2010. **28**(10): p. 1069-78.
101. Ropero, S. and M. Esteller, *The role of histone deacetylases (HDACs) in human cancer*. *Mol Oncol*, 2007. **1**(1): p. 19-25.
102. Fernandes, J.C.R., et al., *Long Non-Coding RNAs in the Regulation of Gene Expression: Physiology and Disease*. *Noncoding RNA*, 2019. **5**(1).
103. Li, Y., et al., *MicroRNA-200b acts as a tumor suppressor in osteosarcoma via targeting ZEB1*. *Onco Targets Ther*, 2016. **9**: p. 3101-11.
104. Jiang, R., et al., *MicroRNA-101 inhibits proliferation, migration and invasion in osteosarcoma cells by targeting ROCK1*. *Am J Cancer Res*, 2017. **7**(1): p. 88-97.
105. Qu, Y., et al., *MicroRNA-150 functions as a tumor suppressor in osteosarcoma by targeting IGF2BP1*. *Tumour Biol*, 2016. **37**(4): p. 5275-84.
106. Luo, Z., et al., *Association of circulating miR-125b and survival in patients with osteosarcoma-A single center experience*. *J Bone Oncol*, 2016. **5**(4): p. 167-172.
107. Xiao, Q., et al., *Overexpression of miR-140 Inhibits Proliferation of Osteosarcoma Cells via Suppression of Histone Deacetylase 4*. *Oncol Res*, 2017. **25**(2): p. 267-275.
108. Xu, H., et al., *miR-574-3p acts as a tumor promoter in osteosarcoma by targeting SMAD4 signaling pathway*. *Oncol Lett*, 2016. **12**(6): p. 5247-5253.
109. Huang, G., et al., *miR-20a encoded by the miR-17-92 cluster increases the metastatic potential of osteosarcoma cells by regulating Fas expression*. *Cancer Res*, 2012. **72**(4): p. 908-16.
110. Xu, H., X. Liu, and J. Zhao, *Down-regulation of miR-3928 promoted osteosarcoma growth*. *Cell Physiol Biochem*, 2014. **33**(5): p. 1547-56.
111. Chen, Y., et al., *LncRNA MALAT1 Promotes Cancer Metastasis in Osteosarcoma via Activation of the PI3K-Akt Signaling Pathway*. *Cell Physiol Biochem*, 2018. **51**(3): p. 1313-1326.
112. Gu, W., et al., *Long noncoding RNA HOXD-AS1 aggravates osteosarcoma carcinogenesis through epigenetically inhibiting p57 via EZH2*. *Biomed Pharmacother*, 2018. **106**: p. 890-895.
113. Guo, W., et al., *LncRNA-SRA1 Suppresses Osteosarcoma Cell Proliferation While Promoting Cell Apoptosis*. *Technol Cancer Res Treat*, 2019. **18**: p. 1533033819841438.
114. Deng, R., J. Zhang, and J. Chen, *lncRNA SNHG1 negatively regulates miRNA1013p to enhance the expression of ROCK1 and promote cell proliferation, migration and invasion in osteosarcoma*. *Int J Mol Med*, 2019. **43**(3): p. 1157-1166.
115. Wu, Y., et al., *Circular RNA circTADA2A promotes osteosarcoma progression and metastasis by sponging miR-203a-3p and regulating CREB3 expression*. *Mol Cancer*, 2019. **18**(1): p. 73.
116. Liu, W., et al., *Microarray Expression Profile and Functional Analysis of Circular RNAs in Osteosarcoma*. *Cell Physiol Biochem*, 2017. **43**(3): p. 969-985.
117. Misdorp, W., *Skeletal osteosarcoma. Animal model: canine osteosarcoma*. *Am J Pathol*, 1980. **98**(1): p. 285-8.
118. Liao, A.T., M. McMahon, and C.A. London, *Identification of a novel germline MET mutation in dogs*. *Anim Genet*, 2006. **37**(3): p. 248-52.
119. Paoloni, M., et al., *Canine tumor cross-species genomics uncovers targets linked to osteosarcoma progression*. *BMC Genomics*, 2009. **10**: p. 625.
120. Ng, A.J., et al., *Genetically engineered mouse models and human osteosarcoma*. *Clin Sarcoma Res*, 2012. **2**(1): p. 19.
121. Guijarro, M.V., S.C. Ghivizzani, and C.P. Gibbs, *Animal models in osteosarcoma*. *Front Oncol*, 2014. **4**: p. 189.

122. Ruther, U., et al., *c-fos expression induces bone tumors in transgenic mice*. *Oncogene*, 1989. **4**(7): p. 861-5.
123. Krimpenfort, P., et al., *p15Ink4b is a critical tumour suppressor in the absence of p16Ink4a*. *Nature*, 2007. **448**(7156): p. 943-6.
124. Sharpless, N.E., et al., *Loss of p16Ink4a with retention of p19Arf predisposes mice to tumorigenesis*. *Nature*, 2001. **413**(6851): p. 86-91.
125. Martin-Caballero, J., et al., *Tumor susceptibility of p21(Waf1/Cip1)-deficient mice*. *Cancer Res*, 2001. **61**(16): p. 6234-8.
126. Cobb, L.M., *Radiation-induced osteosarcoma in the rat as a model for osteosarcoma in man*. *Br J Cancer*, 1970. **24**(2): p. 294-9.
127. Cherrier, B., et al., *A new experimental rat model of osteosarcoma established by intrafemoral tumor cell inoculation, useful for biology and therapy investigations*. *Tumour Biol*, 2005. **26**(3): p. 121-30.
128. Yu, Z., et al., *Establishment of reproducible osteosarcoma rat model using orthotopic implantation technique*. *Oncol Rep*, 2009. **21**(5): p. 1175-80.
129. Sieren, J.C., et al., *Development and translational imaging of a TP53 porcine tumorigenesis model*. *J Clin Invest*, 2014. **124**(9): p. 4052-66.
130. Leuchs, S., et al., *Inactivation and inducible oncogenic mutation of p53 in gene targeted pigs*. *PLoS One*, 2012. **7**(10): p. e43323.
131. Saalfrank, A., et al., *A porcine model of osteosarcoma*. *Oncogenesis*, 2016. **5**: p. e210.
132. Lannagan, T.R., et al., *Advances in colon cancer research: in vitro and animal models*. *Curr Opin Genet Dev*, 2021. **66**: p. 50-56.
133. Muller, M.F., A.E. Ibrahim, and M.J. Arends, *Molecular pathological classification of colorectal cancer*. *Virchows Arch*, 2016. **469**(2): p. 125-34.
134. Trobaugh-Lotrario, A.D., et al., *Hepatoblastoma in patients with molecularly proven familial adenomatous polyposis: Clinical characteristics and rationale for surveillance screening*. *Pediatr Blood Cancer*, 2018. **65**(8): p. e27103.
135. Flisikowska, T., et al., *A porcine model of familial adenomatous polyposis*. *Gastroenterology*, 2012. **143**(5): p. 1173-1175 e7.
136. Esteller, M., et al., *Analysis of adenomatous polyposis coli promoter hypermethylation in human cancer*. *Cancer Res*, 2000. **60**(16): p. 4366-71.
137. Li, B.Q., P.P. Liu, and C.H. Zhang, *Correlation between the methylation of APC gene promoter and colon cancer*. *Oncol Lett*, 2017. **14**(2): p. 2315-2319.
138. Michael, M.Z., et al., *Reduced accumulation of specific microRNAs in colorectal neoplasia*. *Mol Cancer Res*, 2003. **1**(12): p. 882-91.
139. Roshani Asl, E., Y. Rasmi, and B. Baradaran, *MicroRNA-124-3p suppresses PD-L1 expression and inhibits tumorigenesis of colorectal cancer cells via modulating STAT3 signaling*. *J Cell Physiol*, 2021. **236**(10): p. 7071-7087.
140. Flisikowski, K., et al., *Wild-type APC Influences the Severity of Familial Adenomatous Polyposis*. *Cell Mol Gastroenterol Hepatol*, 2022. **13**(2): p. 669-671 e3.
141. Deng, S., et al., *Over-expressed miRNA-200b ameliorates ulcerative colitis-related colorectal cancer in mice through orchestrating epithelial-mesenchymal transition and inflammatory responses by channel of AKT2*. *Int Immunopharmacol*, 2018. **61**: p. 346-354.
142. Du, F., et al., *KRAS Mutation-Responsive miR-139-5p inhibits Colorectal Cancer Progression and is repressed by Wnt Signaling*. *Theranostics*, 2020. **10**(16): p. 7335-7350.
143. Yang, X.D., et al., *Knockdown of long non-coding RNA HOTAIR inhibits proliferation and invasiveness and improves radiosensitivity in colorectal cancer*. *Oncol Rep*, 2016. **35**(1): p. 479-87.
144. Silva-Fisher, J.M., et al., *Long non-coding RNA RAMS11 promotes metastatic colorectal cancer progression*. *Nat Commun*, 2020. **11**(1): p. 2156.
145. Pichler, M., et al., *Therapeutic potential of FLANC, a novel primate-specific long non-coding RNA in colorectal cancer*. *Gut*, 2020. **69**(10): p. 1818-1831.

146. Wang, M., et al., *Long non-coding RNA H19 confers 5-Fu resistance in colorectal cancer by promoting SIRT1-mediated autophagy*. *Cell Death Dis*, 2018. **9**(12): p. 1149.
147. Wu, M., et al., *Hsa_circRNA_002144 promotes growth and metastasis of colorectal cancer through regulating miR-615-5p/LARP1/mTOR pathway*. *Carcinogenesis*, 2021. **42**(4): p. 601-610.
148. Chen, J., et al., *CircRNA ciRS-7: a Novel Oncogene in Multiple Cancers*. *Int J Biol Sci*, 2021. **17**(1): p. 379-389.
149. Lu, H., et al., *FBXW7 circular RNA regulates proliferation, migration and invasion of colorectal carcinoma through NEK2, mTOR, and PTEN signaling pathways in vitro and in vivo*. *BMC Cancer*, 2019. **19**(1): p. 918.
150. Lisco, H., M.P. Finkel, and A.M. Brues, *Carcinogenic properties of radioactive fission products and of plutonium*. *Radiology*, 1947. **49**(3): p. 361-3.
151. Liu, Z.Y., et al., *Two water-bridged cobalt(II) chains with isomeric naphthoate spacers: from metamagnetic to single-chain magnetic behaviour*. *Dalton Trans*, 2015. **44**(46): p. 19927-34.
152. Moser, A.R., H.C. Pitot, and W.F. Dove, *A dominant mutation that predisposes to multiple intestinal neoplasia in the mouse*. *Science*, 1990. **247**(4940): p. 322-4.
153. Yamada, Y. and H. Mori, *Multistep carcinogenesis of the colon in Apc(Min/+) mouse*. *Cancer Sci*, 2007. **98**(1): p. 6-10.
154. Colnot, S., et al., *Colorectal cancers in a new mouse model of familial adenomatous polyposis: influence of genetic and environmental modifiers*. *Lab Invest*, 2004. **84**(12): p. 1619-30.
155. Crist, R.C., et al., *The armadillo repeat domain of Apc suppresses intestinal tumorigenesis*. *Mamm Genome*, 2010. **21**(9-10): p. 450-7.
156. Oshima, M., et al., *Loss of Apc heterozygosity and abnormal tissue building in nascent intestinal polyps in mice carrying a truncated Apc gene*. *Proc Natl Acad Sci U S A*, 1995. **92**(10): p. 4482-6.
157. Fazeli, A., et al., *Effects of p53 mutations on apoptosis in mouse intestinal and human colonic adenomas*. *Proc Natl Acad Sci U S A*, 1997. **94**(19): p. 10199-204.
158. Sansom, O.J., et al., *Loss of Apc allows phenotypic manifestation of the transforming properties of an endogenous K-ras oncogene in vivo*. *Proc Natl Acad Sci U S A*, 2006. **103**(38): p. 14122-7.
159. Hung, K.E., et al., *Development of a mouse model for sporadic and metastatic colon tumors and its use in assessing drug treatment*. *Proc Natl Acad Sci U S A*, 2010. **107**(4): p. 1565-70.
160. Sancho, R., et al., *F-box and WD repeat domain-containing 7 regulates intestinal cell lineage commitment and is a haploinsufficient tumor suppressor*. *Gastroenterology*, 2010. **139**(3): p. 929-41.
161. Burtin, F., C.S. Mullins, and M. Linnebacher, *Mouse models of colorectal cancer: Past, present and future perspectives*. *World J Gastroenterol*, 2020. **26**(13): p. 1394-1426.
162. Amos-Landgraf, J.M., et al., *A target-selected Apc-mutant rat kindred enhances the modeling of familial human colon cancer*. *Proc Natl Acad Sci U S A*, 2007. **104**(10): p. 4036-41.
163. Yoshimi, K., et al., *Enhanced colitis-associated colon carcinogenesis in a novel Apc mutant rat*. *Cancer Sci*, 2009. **100**(11): p. 2022-7.
164. Irving, A.A., et al., *The utility of Apc-mutant rats in modeling human colon cancer*. *Dis Model Mech*, 2014. **7**(11): p. 1215-25.
165. Flisikowska, T., et al., *Porcine familial adenomatous polyposis model enables systematic analysis of early events in adenoma progression*. *Sci Rep*, 2017. **7**(1): p. 6613.
166. Bray, N.L., et al., *Near-optimal probabilistic RNA-seq quantification*. *Nat Biotechnol*, 2016. **34**(5): p. 525-7.
167. Pimentel, H., et al., *Differential analysis of RNA-seq incorporating quantification uncertainty*. *Nat Methods*, 2017. **14**(7): p. 687-690.

168. Niu, G., et al., *Porcine model elucidates function of p53 isoform in carcinogenesis and reveals novel circTP53 RNA*. *Oncogene*, 2021.
169. Niu, G., et al., *Allelic Expression Imbalance Analysis Identified YAP1 Amplification in p53- Dependent Osteosarcoma*. *Cancers (Basel)*, 2021. **13**(6).
170. Bourdon, J.C., et al., *p53 isoforms can regulate p53 transcriptional activity*. *Genes Dev*, 2005. **19**(18): p. 2122-37.
171. Jorruiz, S.M. and J.C. Bourdon, *p53 Isoforms: Key Regulators of the Cell Fate Decision*. *Cold Spring Harb Perspect Med*, 2016. **6**(8).
172. Fujita, K., et al., *p53 isoforms Delta133p53 and p53beta are endogenous regulators of replicative cellular senescence*. *Nat Cell Biol*, 2009. **11**(9): p. 1135-42.
173. Bernard, H., et al., *The p53 isoform, Delta133p53alpha, stimulates angiogenesis and tumour progression*. *Oncogene*, 2013. **32**(17): p. 2150-60.
174. Slatter, T.L., et al., *Delta122p53, a mouse model of Delta133p53alpha, enhances the tumor-suppressor activities of an attenuated p53 mutant*. *Cell Death Dis*, 2015. **6**: p. e1783.
175. Slatter, T.L., et al., *Hyperproliferation, cancer, and inflammation in mice expressing a Delta133p53-like isoform*. *Blood*, 2011. **117**(19): p. 5166-77.
176. Campbell, H.G., et al., *Does Delta133p53 isoform trigger inflammation and autoimmunity?* *Cell Cycle*, 2012. **11**(3): p. 446-50.
177. Vodicka, P., et al., *The miniature pig as an animal model in biomedical research*. *Ann N Y Acad Sci*, 2005. **1049**: p. 161-71.
178. Verma, N., A.W. Rettenmeier, and S. Schmitz-Spanke, *Recent advances in the use of Sus scrofa (pig) as a model system for proteomic studies*. *Proteomics*, 2011. **11**(4): p. 776-93.
179. Bykov, V.J.N., et al., *Targeting mutant p53 for efficient cancer therapy*. *Nat Rev Cancer*, 2018. **18**(2): p. 89-102.
180. Fragou, A., et al., *Increased Delta133p53 mRNA in lung carcinoma corresponds with reduction of p21 expression*. *Mol Med Rep*, 2017. **15**(4): p. 1455-1460.
181. Hofstetter, G., et al., *Delta133p53 is an independent prognostic marker in p53 mutant advanced serous ovarian cancer*. *Br J Cancer*, 2011. **105**(10): p. 1593-9.
182. Nutthasirikul, N., et al., *Ratio disruption of the 133p53 and TAp53 isoform equilibrium correlates with poor clinical outcome in intrahepatic cholangiocarcinoma*. *Int J Oncol*, 2013. **42**(4): p. 1181-8.
183. Avery-Kiejda, K.A., et al., *The relative mRNA expression of p53 isoforms in breast cancer is associated with clinical features and outcome*. *Carcinogenesis*, 2014. **35**(3): p. 586-96.
184. Candeias, M.M., M. Hagiwara, and M. Matsuda, *Cancer-specific mutations in p53 induce the translation of Delta160p53 promoting tumorigenesis*. *EMBO Rep*, 2016. **17**(11): p. 1542-1551.
185. Stindt, M.H., et al., *Functional interplay between MDM2, p63/p73 and mutant p53*. *Oncogene*, 2015. **34**(33): p. 4300-10.
186. Zhang, J., et al., *Mutant p53 antagonizes p63/p73-mediated tumor suppression via Notch1*. *Proc Natl Acad Sci U S A*, 2019. **116**(48): p. 24259-24267.
187. Gonfloni, S., V. Caputo, and V. Iannizzotto, *P63 in health and cancer*. *Int J Dev Biol*, 2015. **59**(1-3): p. 87-93.
188. Lucena-Araujo, A.R., et al., *High DeltaNp73/TAp73 ratio is associated with poor prognosis in acute promyelocytic leukemia*. *Blood*, 2015. **126**(20): p. 2302-6.
189. Tomasini, R., et al., *TAp73 knockout shows genomic instability with infertility and tumor suppressor functions*. *Genes Dev*, 2008. **22**(19): p. 2677-91.
190. Wilhelm, M.T., et al., *Isoform-specific p73 knockout mice reveal a novel role for delta Np73 in the DNA damage response pathway*. *Genes Dev*, 2010. **24**(6): p. 549-60.
191. Wang, C., et al., *Emerging Roles of Circular RNAs in Osteosarcoma*. *Med Sci Monit*, 2018. **24**: p. 7043-7050.
192. Reimann, E., et al., *Whole exome sequencing of a single osteosarcoma case-- integrative analysis with whole transcriptome RNA-seq data*. *Hum Genomics*, 2014. **8**: p. 20.

193. Montgomery, S.B., et al., *Transcriptome genetics using second generation sequencing in a Caucasian population*. Nature, 2010. **464**(7289): p. 773-7.
194. Lappalainen, T., et al., *Transcriptome and genome sequencing uncovers functional variation in humans*. Nature, 2013. **501**(7468): p. 506-11.
195. Pickrell, J.K., et al., *Understanding mechanisms underlying human gene expression variation with RNA sequencing*. Nature, 2010. **464**(7289): p. 768-72.
196. Castel, S.E., et al., *Tools and best practices for data processing in allelic expression analysis*. Genome Biol, 2015. **16**: p. 195.
197. Liu, Z., X. Dong, and Y. Li, *A Genome-Wide Study of Allele-Specific Expression in Colorectal Cancer*. Front Genet, 2018. **9**: p. 570.
198. Pastinen, T., *Genome-wide allele-specific analysis: insights into regulatory variation*. Nat Rev Genet, 2010. **11**(8): p. 533-8.
199. Atiye, J., et al., *Gene amplifications in osteosarcoma-CGH microarray analysis*. Genes Chromosomes Cancer, 2005. **42**(2): p. 158-63.
200. Fernandez, L.A., et al., *YAP1 is amplified and up-regulated in hedgehog-associated medulloblastomas and mediates Sonic hedgehog-driven neural precursor proliferation*. Genes Dev, 2009. **23**(23): p. 2729-41.
201. Shih, D.J.H., et al., *Genomic characterization of human brain metastases identifies drivers of metastatic lung adenocarcinoma*. Nat Genet, 2020. **52**(4): p. 371-377.
202. Dai, H., et al., *YAP1 amplification as a prognostic factor of definitive chemoradiotherapy in nonsurgical esophageal squamous cell carcinoma*. Cancer Med, 2020. **9**(5): p. 1628-1637.
203. Mello, S.S., et al., *A p53 Super-tumor Suppressor Reveals a Tumor Suppressive p53-Ptpn14-Yap Axis in Pancreatic Cancer*. Cancer Cell, 2017. **32**(4): p. 460-473 e6.
204. Murakami, S., et al., *A Yap-Myc-Sox2-p53 Regulatory Network Dictates Metabolic Homeostasis and Differentiation in Kras-Driven Pancreatic Ductal Adenocarcinomas*. Dev Cell, 2019. **51**(1): p. 113-128 e9.
205. Zhang, W., et al., *Downstream of mutant KRAS, the transcription regulator YAP is essential for neoplastic progression to pancreatic ductal adenocarcinoma*. Sci Signal, 2014. **7**(324): p. ra42.
206. Di Agostino, S., et al., *YAP enhances the pro-proliferative transcriptional activity of mutant p53 proteins*. EMBO Rep, 2016. **17**(2): p. 188-201.
207. Mao, Y., S. Sun, and K.D. Irvine, *Role and regulation of Yap in KrasG12D-induced lung cancer*. Oncotarget, 2017. **8**(67): p. 110877-110889.
208. Xie, Q., et al., *YAP/TEAD-mediated transcription controls cellular senescence*. Cancer Res, 2013. **73**(12): p. 3615-24.
209. Saladi, S.V., et al., *ACTL6A Is Co-Amplified with p63 in Squamous Cell Carcinoma to Drive YAP Activation, Regenerative Proliferation, and Poor Prognosis*. Cancer Cell, 2017. **31**(1): p. 35-49.
210. Strano, S., et al., *The transcriptional coactivator Yes-associated protein drives p73 gene-target specificity in response to DNA Damage*. Mol Cell, 2005. **18**(4): p. 447-59.

ACKNOWLEDGEMENT

The whole study was conducted in the Chair of livestock biotechnology, department of animal science, school of life science, Technical University of Munich, Freising, Germany. It was my great honor to be a member of this group. Now I would like to give my special thanks to my supervisor, mentor, colleagues and friends.

First of all, I would like to give my thanks to my supervisor Prof. Dr. Angelika Schnieke for offering me the chance to pursue my PhD in this chair. Her extensive knowledge and rigorous approach to research really inspires me. Her constant encouragement, valuable ideas and suggestions contributed to the success of the whole project.

Special thanks go to Dr. Krzysztof Flisikowski. Actually, I do not know how much thanks I should give him for both my scientific career and life in general. It is beyond my power of description. His wisdom, humor and patience provided the base for the success of my doctoral study.

I thank Dr. Tatiana Flisikowska for her help with my work and daily life. I still remember that she took me to the supermarket at my first day in Germany. I thank Dr. Alex Kind for his help in improving my English. I thank Dr. Beate Rieblinger and Dr. Bernhard Klinger for help with practical work and suggestions for writing my thesis. I thank Dr. Konrad Fisher for his support with new methods.

I thank Sulith for lab assistance, Sulith knows everything in the lab and is always willing to offer help. I thank Alex, he is such a nice man that whenever I need something, I would say 'Alex...'. I thank Barbara, Peggy, Marlene, Kristina, Johanna for help in the lab and life.

My fellow PhD students: Wei Liang, thanks for your help and support during my whole PhD. Dani Kalla, three years my office mate, and Aga; to both of you my thanks for the help in science and life. Alessandro, thanks for the great help in the lab including sample searching. Thomas, here I would say '谢谢', David, thanks for the help. Yue Zhang, Ying Wang, Yajun Wang, Yiduan Liu and Meli, thanks for the help in the lab and daily life.

I also like to thank Prof. Dr. Benjamin Schusser and his people from the "chicken group".

I would like to give my thanks to my Chinese friends and roommates in Freising, who made it a pleasant stay in Germany during my PhD.

Great thanks should be given to my family, my parents, sisters and friends, thanks for your support that giving me the courage to move towards to a nicer future.